Mathematical Biosciences 264 (2015) 128–144

Contents lists available at ScienceDirect

Mathematical Biosciences

journal homepage: www.elsevier.com/locate/mbs

Modeling malaria and typhoid fever co-infection dynamics

Jones M. Mutua [a], Feng-Bin Wang [b], Naveen K. Vaidya [a,*]

[a] Department of Mathematics and Statistics, University of Missouri–Kansas City, Kansas City, MO 64110, USA
[b] Department of Natural Science in the Center for General Education, Chang Gung University, Kwei-Shan, Taoyuan 333, Taiwan

ARTICLE INFO

Article history:
Received 11 December 2014
Revised 25 March 2015
Accepted 27 March 2015
Available online 10 April 2015

Keywords:
Co-infection
Malaria
Typhoid
False diagnosis
Mathematical analysis
Reproduction numbers

ABSTRACT

Malaria and typhoid are among the most endemic diseases, and thus, of major public health concerns in tropical developing countries. In addition to true co-infection of malaria and typhoid, false diagnoses due to similar signs and symptoms and false positive results in testing methods, leading to improper controls, are the major challenges on managing these diseases. In this study, we develop novel mathematical models describing the co-infection dynamics of malaria and typhoid. Through mathematical analyses of our models, we identify distinct features of typhoid and malaria infection dynamics as well as relationships associated to their co-infection. The global dynamics of typhoid can be determined by a single threshold (the typhoid basic reproduction number, $\mathcal{R}_0^T$) while two thresholds (the malaria basic reproduction number, $\mathcal{R}_0^M$, and the extinction index, $\mathcal{R}_0^{MM}$) are needed to determine the global dynamics of malaria. We demonstrate that by using efficient simultaneous prevention programs, the co-infection basic reproduction number, $\mathcal{R}_0$, can be brought down to below one, thereby eradicating the diseases. Using our model, we present illustrative numerical results with a case study in the Eastern Province of Kenya to quantify the possible false diagnosis resulting from this co-infection. In Kenya, despite having higher prevalence of typhoid, malaria is more problematic in terms of new infections and disease deaths. We find that false diagnosis—with higher possible cases for typhoid than malaria—cause significant devastating impacts on Kenyan societies. Our results demonstrate that both diseases need to be simultaneously managed for successful control of co-epidemics.

1. Introduction

Over the past three to four decades, malaria has been a major cause of death and illness among children and adults in many developing countries. Approximately 300–500 million cases occur worldwide each year, with more than a million annual deaths [5,36,49]. About 80% of these cases and 90% of these deaths occur in Sub-Saharan Africa [16,19,44]. While malaria is already causing devastating impacts on the tropical developing countries, typhoid fever is quite common in the malaria affected areas, thereby drastically exacerbating the public health burden. Worldwide, over 21 million cases and more than a half million typhoid related deaths occur each year, with most of them taking place in Africa [2,11,23,31]. While people in tropical communities are living at risk of contracting both diseases (either concurrently or an acute infection superimposed on a chronic one [10]), misleading diagnosis due to similar symptoms of these diseases and incompetent testing methodologies is one of the biggest challenges for their control [16,44]. Thus studies of malaria and typhoid are becoming increasingly important.

Malaria is acquired and transmitted to humans through bites by infected anopheles mosquitoes, whereas typhoid is caused by the gram-negative-bacterium of the genus salmonella [16,50], known as *Salmonella Typhi*, through ingestion of foods and drinks contaminated by infected waste. Despite differences in causes and routes of transmission, malaria and typhoid have interesting relationships causing public health encumber, which can be discussed in two broad categories: real co-infection and false diagnosis.

It is known that anemia occurs in malaria infected individuals resulting in excessive deposition of iron in the liver, which supports the growth of salmonella bacteria that causes typhoid fever [8,36]. Moreover, malaria infected individuals suffer from deficiency of complements such as C3, C4, and C19 [36], and the complement deficiency causes an enhanced susceptibility to salmonella infection [9,48]. Therefore, infection due to malaria leads to an increased susceptibility of typhoid. Complements are consumed during malaria infection, impairing host defense mechanisms thereby slowing down any anticipated disease recovery [34]. Furthermore, co-infected individuals have a higher chance of dying because of infections due to both diseases.

While real malaria–typhoid co-infections mentioned above pose significant problems, false diagnosis often resulting in mismanagement of these diseases remains one of the biggest public health

* Corresponding author. Tel.: +18162352847; fax: +18162355517.
E-mail address: vaidyan@umkc.edu (N.K. Vaidya).

http://dx.doi.org/10.1016/j.mbs.2015.03.014
0025-5564/

burdens. Malaria and typhoid exhibit similar signs and symptoms such as fever, headache, vomiting, diarrhoea, and abdominal and muscle pain among others [21,33]. This, in many cases, entices physicians to relate these signs and symptoms with a wrong disease, leading to false diagnosis. Moreover, many existing testing methods, including the most commonly used Widal test [2], frequently generate false positive results. For example, in one study [16] the Widal test showed about 57% of typhoid positive cases whereas truly only 15% were found to have typhoid when more reliable bacteria-culture tests were performed. Despite being more accurate, the bacteria-culture test is not commonly used in practice because of higher costs and longer processing time [36]. This high likelihood of typhoid false positive results in malaria patients from the Widal test is due to a cross reaction between malaria parasites and typhoid antigens [36]. Such false diagnoses may lead to mismanagement of these diseases, posing a vast challenge toward controlling them. For instance, giving antibiotics to seemingly typhoid patients, when they actually have malaria, not only leads to waste of drugs but also may cause emergence of drug resistance in the event of true future typhoid infection. It is thus critical to understand the impact of real co-infection as well as false diagnosis on the disease dynamics.

Mathematical modeling of malaria dynamics is quite advanced [4,6,13,14,26,28]. However, modeling of typhoid fever is very limited [1,30]. While these existing models have provided significant insights into the understanding of individual disease dynamics, they need to be considered simultaneously for devising proper strategies to mitigate both disease burdens. Recently, a study [29] has provided a malaria–typhoid co-infection model, which only considers direct transmission of typhoid (person-to-person) and assumes no recovery of co-infected individuals from single diseases. In this study, we first develop an improved realistic typhoid model. Then based on our new typhoid model and existing standard malaria model, we further develop a co-infection model that captures the dynamics of malaria and typhoid together. Using our model, we develop a formula for the co-infection basic reproduction number, and compare it with the basic reproduction number of individual diseases. We analyze the models for stability of equilibria and persistence of diseases. Furthermore, using parameters relevant to the Eastern Province of Kenya, we study real co-infection dynamics and estimate the possible false diagnosis which poses a big challenge to controlling these diseases.

2. Model formulation

We first develop a more realistic model for typhoid. The model subdivides the human population of interest into four compartments: susceptible humans (S), infected humans (I), carrier humans (C), and recovered humans (R). Previous models of typhoid dynamics [1,29,30], including the one describing malaria–typhoid co-infection [29], assume direct transmission of typhoid from infected individuals to susceptible individuals. However, typhoid is largely contracted from environmental bacteria through contaminated water and/or food and drinks [7,44], and transmission of typhoid through direct person-to-person contact, if any, is negligible [20,47]. To incorporate this real biological phenomena, we consider an additional compartment, B, which represents bacteria in the environment. We assume that susceptible individuals get infected with typhoid at a rate proportional to the susceptible population, S, and the environmental bacteria concentration, B, at a constant rate β. The infected individuals either progress to carrier class, C, at rate α_t or recover at rate η. Individuals in the carrier class can also recover from typhoid, but with a significantly slow rate, γ. Infected individuals in both infectious state and carrier state excrete bacteria into the environment. However, the rate of excretion by the infectious group, p_i, is significantly higher than that by the carrier group, p_c. Note that despite low excretion of bacteria by the carrier group, because of its extremely long duration without showing any sickness the carrier group plays an important role on co-infection dynamics of malaria and typhoid. Growth curves of organisms are often described well with the logistic models [17,22,32,35,45], so we assume that the bacteria in the environment grows according to a logistic growth rate and becomes non-infectious at a rate μ_b. r and κ represent per capita growth rate and carrying capacity, respectively, and λ denotes the typhoid induced mortality in humans. The constant recruitment rate into the susceptible human is represented by Λ_h, while the natural death rate of human is represented by μ_h. The developed model can be expressed as the following differential equations.

$$\begin{aligned}
\frac{dS}{dt} &= \Lambda_h - (\beta B + \mu_h) S,\\
\frac{dI}{dt} &= \beta BS - (\mu_h + \lambda + \alpha_t + \eta) I,\\
\frac{dC}{dt} &= \alpha_t I - (\mu_h + \gamma) C,\\
\frac{dR}{dt} &= \eta I + \gamma C - \mu_h R,\\
\frac{dB}{dt} &= rB\left(1 - \frac{B}{\kappa}\right) + p_i I + p_c C - \mu_b B.
\end{aligned} \tag{2.1}$$

Similar to the previous studies [4,6,13,14,15,26,28], we consider a malaria model consisting of four human compartments (susceptible, S, exposed, E, infected, I, and recovered, R) and three mosquito compartments (susceptible, S_m, exposed, E_m, and infected, I_m). In this model, new infected humans are generated by mosquito-bites at an effective biting rate, $\alpha_{mh} b_m$, where α_{mh} denotes the infection probability, per bite, from an infectious mosquito to a susceptible human and b_m denotes the total number of mosquito bites per mosquito per day. Similarly, new infected mosquitoes are generated at an effective biting rate, $\alpha_{hm} b_m$, when susceptible mosquitoes bite infected humans. Here, α_{hm} denotes the probability of successful transmission of malaria from the human to the mosquito, per mosquito bite. The rates at which humans and mosquitoes progress from the exposed class to the infectious class are denoted by δ_h and γ_m, respectively. We define α_h as the rate at which individuals infected with malaria recover from the disease and ω as the malaria induced mortality in humans. The constant recruitment rate into the mosquito populations is represented by Λ_m, while the death rate of mosquito populations is represented by μ_m, respectively. The model we study is as follows:

$$\begin{aligned}
\frac{dS}{dt} &= \Lambda_h - \frac{\alpha_{mh} b_m I_m}{N_h} S - \mu_h S,\\
\frac{dE}{dt} &= \frac{\alpha_{mh} b_m I_m}{N_h} S - (\mu_h + \delta_h) E,\\
\frac{dI}{dt} &= \delta_h E - (\mu_h + \alpha_h + \omega) I,\\
\frac{dR}{dt} &= \alpha_h I - \mu_h R,\\
\frac{dS_m}{dt} &= \Lambda_m - \mu_m S_m - \frac{\alpha_{hm} b_m I}{N_h} S_m,\\
\frac{dE_m}{dt} &= \frac{\alpha_{hm} b_m I}{N_h} S_m - (\mu_m + \gamma_m) E_m,\\
\frac{dI_m}{dt} &= \gamma_m E_m - \mu_m I_m.
\end{aligned} \tag{2.2}$$

Based on our novel typhoid model (2.1) and existing malaria model (2.2), we now develop a co-infection model using the four states of typhoid and the four states of malaria. A schematic diagram of the model is shown in Fig. 1. The total human population is therefore subdivided into sixteen mutually exclusive, collectively exhaustive compartments: typhoid-susceptible and malaria-susceptible (X_{SS}); typhoid-susceptible and malaria-exposed (X_{SE}); typhoid-susceptible and malaria-infected (X_{SI});

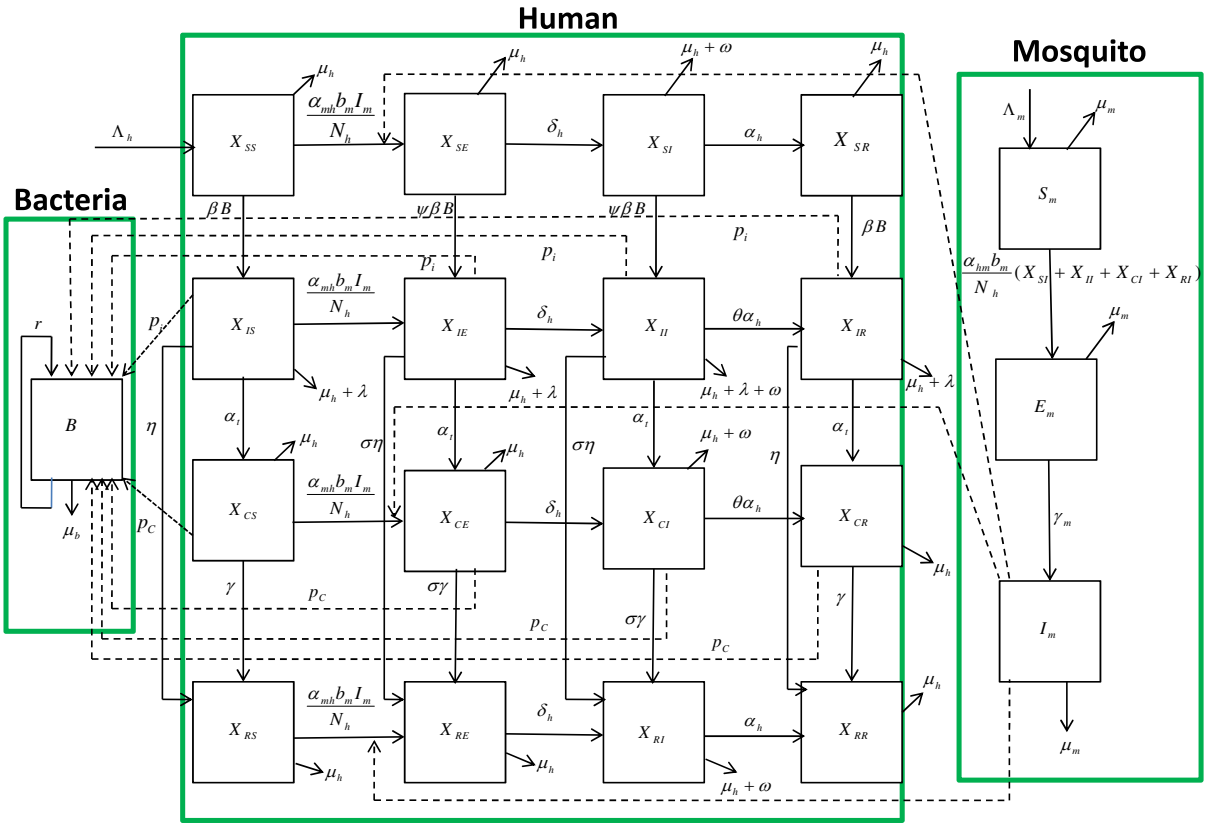

Fig. 1. A schematic diagram of co-infection model.

typhoid-susceptible and malaria-recovered (X_{SR}); typhoid-infected and malaria-susceptible (X_{IS}); typhoid-infected and malaria-exposed (X_{IE}); typhoid-infected and malaria-infected (X_{II}); typhoid-infected and malaria-recovered (X_{IR}); typhoid-carrier and malaria-susceptible (X_{CS}); typhoid-carrier and malaria-exposed (X_{CE}); typhoid-carrier and malaria-infected (X_{CI}); typhoid-carrier and malaria-recovered (X_{CR}); typhoid-recovered and malaria-susceptible (X_{RS}); typhoid-recovered and malaria-exposed (X_{RE}); typhoid-recovered and malaria-infected (X_{RI}); and typhoid-recovered and malaria-recovered (X_{RR}). The first subscript of each compartment is assigned to a typhoid state, and the second subscript to a malaria state. In addition, we consider a compartment, B, representing the bacteria concentration in the environment, and three vector compartments, S_m, E_m, and I_m, representing susceptible, exposed, and infected mosquito populations, respectively. Our full co-infection model thus contains the following 20 differential equations.

$$
\begin{aligned}
\frac{dX_{SS}}{dt} &= \Lambda_h - \beta B X_{SS} - \frac{\alpha_{mh} b_m I_m X_{SS}}{N_h} - \mu_h X_{SS},\\
\frac{dX_{SE}}{dt} &= \frac{\alpha_{mh} b_m I_m X_{SS}}{N_h} - (\mu_h + \delta_h + \psi\beta B) X_{SE},\\
\frac{dX_{SI}}{dt} &= \delta_h X_{SE} - (\mu_h + \alpha_h + \omega + \psi\beta B) X_{SI},\\
\frac{dX_{SR}}{dt} &= \alpha_h X_{SI} - (\mu_h + \beta B) X_{SR},\\
\frac{dX_{IS}}{dt} &= \beta B X_{SS} - \frac{\alpha_{mh} b_m I_m}{N_h} X_{IS} - (\mu_h + \lambda + \alpha_t + \eta) X_{IS},\\
\frac{dX_{IE}}{dt} &= \frac{\alpha_{mh} b_m I_m}{N_h} X_{IS} + \psi\beta B X_{SE} - (\mu_h + \lambda + \delta_h + \alpha_t + \sigma\eta) X_{IE},\\
\frac{dX_{II}}{dt} &= \delta_h X_{IE} + \psi\beta B X_{SI} - (\mu_h + \lambda + \omega + \alpha_t + \sigma\eta + \theta\alpha_h) X_{II},\\
\frac{dX_{IR}}{dt} &= \theta\alpha_h X_{II} + \beta B X_{SR} - (\mu_h + \lambda + \alpha_t + \eta) X_{IR},\\
\frac{dX_{CS}}{dt} &= \alpha_t X_{IS} - \frac{\alpha_{mh} b_m I_m}{N_h} X_{CS} - (\mu_h + \gamma) X_{CS},\\
\frac{dX_{CE}}{dt} &= \frac{\alpha_{mh} b_m I_m}{N_h} X_{CS} + \alpha_t X_{IE} - (\mu_h + \delta_h + \sigma\gamma) X_{CE},\\
\frac{dX_{CI}}{dt} &= \delta_h X_{CE} + \alpha_t X_{II} - (\mu_h + \omega + \sigma\gamma + \theta\alpha_h) X_{CI},\\
\frac{dX_{CR}}{dt} &= \theta\alpha_h X_{CI} + \alpha_t X_{IR} - (\mu_h + \gamma) X_{CR},\\
\frac{dX_{RS}}{dt} &= \gamma X_{CS} + \eta X_{IS} - \frac{\alpha_{mh} b_m I_m}{N_h} X_{RS} - \mu_h X_{RS},\\
\frac{dX_{RE}}{dt} &= \frac{\alpha_{mh} b_m I_m}{N_h} X_{RS} + \sigma\gamma X_{CE} + \sigma\eta X_{IE} - (\mu_h + \delta_h) X_{RE},\\
\frac{dX_{RI}}{dt} &= \delta_h X_{RE} + \sigma\gamma X_{CI} + \sigma\eta X_{II} - (\mu_h + \alpha_h + \omega) X_{RI},\\
\frac{dX_{RR}}{dt} &= \alpha_h X_{RI} + \gamma X_{CR} + \eta X_{IR} - \mu_h X_{RR},\\
\frac{dB}{dt} &= rB\left(1 - \frac{B}{\kappa}\right) + p_i (X_{IS} + X_{IE} + X_{II} + X_{IR})\\
&\quad + p_c (X_{CS} + X_{CE} + X_{CI} + X_{CR}) - \mu_b B,\\
\frac{dS_m}{dt} &= \Lambda_m - \frac{\alpha_{hm} b_m (X_{SI} + X_{II} + X_{CI} + X_{RI})}{N_h} S_m - \mu_m S_m,\\
\frac{dE_m}{dt} &= \frac{\alpha_{hm} b_m (X_{SI} + X_{II} + X_{CI} + X_{RI})}{N_h} S_m - (\mu_m + \gamma_m) E_m,\\
\frac{dI_m}{dt} &= \gamma_m E_m - \mu_m I_m.
\end{aligned}
\tag{2.3}
$$

The number of people in each compartment at time t is denoted by $X_j(t)$, where $j = SS, SE, SI, SR, IS, IE, II, IR, CS, CE, CI, CR, RS, RE,$

RI, RR. Similarly, the number of mosquitoes in each of the vector compartments at time t is denoted by $S_m(t)$, $E_m(t)$, and $I_m(t)$, while the bacteria in the environment at time t is denoted by $B(t)$. The total human population size at time t is $N_h(t) = X_{SS}(t) + X_{SE}(t) + X_{SI}(t) + X_{SR}(t) + X_{IS}(t) + X_{IE}(t) + X_{II}(t) + X_{IR}(t) + X_{CS}(t) + X_{CE}(t) + X_{CI}(t) + X_{CR}(t) + X_{RS}(t) + X_{RE}(t) + X_{RI}(t) + X_{RR}(t)$, whereas the total mosquito population size at time t is $N_m(t) = S_m(t) + E_m(t) + I_m(t)$.

As discussed earlier, deficiency of complements and/or deposition of iron in the liver in malaria infected individuals increase the susceptibility of typhoid [36,37]. To incorporate this effect in our co-infection model, we introduce a parameter $\psi > 1$ to change the typhoid infection rate β to $\psi\beta$ for malaria infected individuals. Individuals infected with both diseases recover at a slower rate as their immune system is compromised and potentially overwhelmed from the infection [48]. These slower rates are denoted by $\sigma < 1$ and $\theta < 1$ for typhoid and malaria, respectively, i.e. we use $\eta \to \sigma\eta$, $\gamma \to \sigma\gamma$, and $\alpha_h \to \theta\alpha_h$ for co-infected populations. Individuals in co-infection class X_{II} die due to infection of both diseases at the rate $\lambda + \omega$. All parameters in our model are nonnegative.

3. Model analysis

Since the co-infection full model of 20 compartments is extremely complex, we make some simplifications for the purpose of mathematical analysis. However, all our simulation results are based on this full model without simplifications. We assume that recovered individuals from one or both diseases remain immune, and thus they do not take part in co-infection dynamics allowing us to decouple recovered classes from the system. We further assume a relatively short duration of malaria exposed classes, and thus ignore these compartments. Therefore a simplified typhoid–malaria co-infection model will reduce to the total of nine compartments resulting in the following differential equations.

$$\begin{aligned}
\frac{dX_{SS}}{dt} &= \Lambda_h - \beta B X_{SS} - \frac{\alpha_{mh} b_m X_{SS}}{N_h} I_m - \mu_h X_{SS},\\
\frac{dX_{SI}}{dt} &= \frac{\alpha_{mh} b_m X_{SS}}{N_h} I_m - (\mu_h + \alpha_h + \omega + \psi\beta B) X_{SI},\\
\frac{dX_{IS}}{dt} &= \beta B X_{SS} - \frac{\alpha_{mh} b_m I_m}{N_h} X_{IS} - (\mu_h + \lambda + \eta + \alpha_t) X_{IS},\\
\frac{dX_{II}}{dt} &= \frac{\alpha_{mh} b_m I_m}{N_h} X_{IS} + \psi\beta B X_{SI} - (\mu_h + \lambda + \omega + \alpha_t + \theta\alpha_h + \sigma\eta) X_{II},\\
\frac{dX_{CS}}{dt} &= \alpha_t X_{IS} - \frac{\alpha_{mh} b_m I_m}{N_h} X_{CS} - (\mu_h + \gamma) X_{CS},\\
\frac{dX_{CI}}{dt} &= \frac{\alpha_{mh} b_m I_m}{N_h} X_{CS} + \alpha_t X_{II} - (\mu_h + \omega + \theta\alpha_h + \sigma\gamma) X_{CI},\\
\frac{dS_m}{dt} &= \Lambda_m - \frac{\alpha_{hm} b_m (X_{SI} + X_{II} + X_{CI}) S_m}{N_h} - \mu_m S_m,\\
\frac{dI_m}{dt} &= \frac{\alpha_{hm} b_m (X_{SI} + X_{II} + X_{CI}) S_m}{N_h} - \mu_m I_m,\\
\frac{dB}{dt} &= rB\left(1 - \frac{B}{\kappa}\right) + p_i (X_{IS} + X_{II}) + p_c (X_{CS} + X_{CI}) - \mu_b B.
\end{aligned} \tag{3.4}$$

Note that this simplified model still captures all the key relationships between typhoid and malaria diseases, and thus allows us to achieve analytical results giving some insights into co-infection dynamics. We now derive $\mathcal{R}_0$, the co-infection basic reproduction number, which is defined as the average number of secondary infections caused by one infectious individual during his or her entire infectious period. We calculate $\mathcal{R}_0$ for the system (3.4) using the next generation operator method [46]. System (3.4) has the following disease-free equilibrium

$$\mathcal{E}_0 = \left(\frac{\Lambda_h}{\mu_h}, 0, 0, 0, 0, 0, \frac{\Lambda_m}{\mu_m}, 0, 0\right).$$

We now introduce the following two matrices:

$$F = \begin{pmatrix}
0 & 0 & 0 & 0 & 0 & h_3 & 0\\
0 & 0 & 0 & 0 & 0 & 0 & h_1\\
0 & 0 & 0 & 0 & 0 & 0 & 0\\
0 & 0 & 0 & 0 & 0 & 0 & 0\\
0 & 0 & 0 & 0 & 0 & 0 & 0\\
h_4 & 0 & h_4 & 0 & h_4 & 0 & 0\\
0 & p_i & p_i & p_c & p_c & 0 & r
\end{pmatrix},$$

$$V = \begin{pmatrix}
h_5 & 0 & 0 & 0 & 0 & 0 & 0\\
0 & h_2 & 0 & 0 & 0 & 0 & 0\\
0 & 0 & h_6 & 0 & 0 & 0 & 0\\
0 & -\alpha_t & 0 & (\mu_h + \gamma) & 0 & 0 & 0\\
0 & 0 & -\alpha_t & 0 & h_7 & 0 & 0\\
0 & 0 & 0 & 0 & 0 & \mu_m & 0\\
0 & 0 & 0 & 0 & 0 & 0 & \mu_b
\end{pmatrix},$$

where $h_1 = \beta\frac{\Lambda_h}{\mu_h}$, $h_2 = \mu_h + \lambda + \eta + \alpha_t$, $h_3 = \alpha_{mh} b_m$, $h_4 = \alpha_{hm} b_m \frac{\Lambda_m}{\mu_m}\frac{\mu_h}{\Lambda_h}$, $h_5 = \mu_h + \alpha_h + \omega$, $h_6 = \mu_h + \lambda + \omega + \sigma\eta + \theta\alpha_h + \alpha_t$, and $h_7 = \mu_h + \omega + \theta\alpha_h + \sigma\gamma$. Then, the basic reproduction number, $\mathcal{R}_0$, which is the spectral radius of the matrix FV^{-1}, is

$$\mathcal{R}_0 := \rho(FV^{-1}) = \max\{\mathcal{R}_0^T, \mathcal{R}_0^M\},$$

where

$$\mathcal{R}_0^T = \frac{a_{33} + \sqrt{a_{33}^2 + 4a_{13}a_{31}}}{2}$$

and

$$\mathcal{R}_0^M = \sqrt{\frac{h_3 h_4}{h_5 \mu_m}}$$

with $a_{31} = \frac{p_i}{h_2} + \frac{p_c\alpha_t}{h_2(\mu_h+\gamma)}$, $a_{32} = \frac{p_c}{\mu_h+\gamma}$, $a_{13} = \frac{h_1}{\mu_b}$, and $a_{33} = \frac{r}{\mu_b}$. As we prove in the following theorem, $\mathcal{R}_0$ provides a threshold criteria for the disease-free equilibrium to be asymptotically stable.

Theorem 1. *The disease-free equilibrium $\mathcal{E}_0$ of (3.4) is locally asymptotically stable if $\mathcal{R}_0 < 1$, and unstable if $\mathcal{R}_0 > 1$.*

Proof. The local stability of $\mathcal{E}_0$ is determined by the Jacobian matrix of (3.4) at $\mathcal{E}_0$:

$$\mathbf{J} = \begin{pmatrix}
-\mu_h & 0 & 0 & 0 & 0 & 0 & 0 & -\alpha_{mh} b_m & -\beta\frac{\Lambda_h}{\mu_h}\\
0 & c_{22} & 0 & 0 & 0 & 0 & 0 & \alpha_{mh} b_m & 0\\
0 & 0 & c_{33} & 0 & 0 & 0 & 0 & 0 & \beta\frac{\Lambda_h}{\mu_h}\\
0 & 0 & 0 & c_{44} & 0 & 0 & 0 & 0 & 0\\
0 & 0 & \alpha_t & 0 & c_{55} & 0 & 0 & 0 & 0\\
0 & 0 & 0 & \alpha_t & 0 & c_{66} & 0 & 0 & 0\\
0 & -h_4 & 0 & -h_4 & 0 & -h_4 & -\mu_m & 0 & 0\\
0 & h_4 & 0 & h_4 & 0 & h_4 & 0 & -\mu_m & 0\\
0 & 0 & p_i & p_i & p_c & p_c & 0 & 0 & (r - \mu_b)
\end{pmatrix},$$

where $c_{22} = -(\mu_h + \alpha_h + \omega)$, $c_{33} = -(\mu_h + \lambda + \eta + \alpha_t)$, $c_{44} = -(\mu_h + \lambda + \omega + \alpha_t + \theta\alpha_h + \sigma\eta)$, $c_{55} = -(\mu_h + \gamma)$, and $c_{66} = -(\mu_h + \omega + \theta\alpha_h + \sigma\gamma)$.

The characteristic polynomial of $\mathbf{J}$ can be determined by

$$\det(\mathbf{J} - \xi I) = (-\mu_h - \xi)(c_{44} - \xi)(c_{66} - \xi)(-\mu_m - \xi)\det(\hat{\mathbf{J}} - \xi I),$$

where

$$\det(\hat{\mathbf{J}}-\xi I)=\det\begin{pmatrix} c_{22}-\xi & 0 & 0 & \alpha_{mh}b_m & 0\\ 0 & c_{33}-\xi & 0 & 0 & \beta\frac{\Lambda_h}{\mu_h}\\ 0 & \alpha_t & c_{55}-\xi & 0 & 0\\ h_4 & 0 & 0 & -\mu_m-\xi & 0\\ 0 & p_i & p_c & 0 & (r-\mu_b)-\xi \end{pmatrix}.$$

By using the properties of determinant, it follows that

$$\det(\hat{\mathbf{J}}-\xi I)=\det\begin{pmatrix} c_{33}-\xi & 0 & \beta\frac{\Lambda_h}{\mu_h} & 0 & 0\\ \alpha_t & c_{55}-\xi & 0 & 0 & 0\\ p_i & p_c & (r-\mu_b)-\xi & 0 & 0\\ 0 & 0 & 0 & c_{22}-\xi & \alpha_{mh}b_m\\ 0 & 0 & 0 & h_4 & -\mu_m-\xi \end{pmatrix},$$

that is,

$$\det(\hat{\mathbf{J}}-\xi I)=\det\begin{pmatrix} c_{33}-\xi & 0 & \beta\frac{\Lambda_h}{\mu_h}\\ \alpha_t & c_{55}-\xi & 0\\ p_i & p_c & (r-\mu_b)-\xi \end{pmatrix}\times\det\begin{pmatrix} c_{22}-\xi & \alpha_{mh}b_m\\ h_4 & -\mu_m-\xi \end{pmatrix}.$$

Therefore, four eigenvalues of $\mathbf{J}$ are $-\mu_h$, c_{44}, c_{66}, and $-\mu_m$, which are all negative, and the remaining five eigenvalues are given by the solution of the following equations:

$$\det\begin{pmatrix} c_{33}-\xi & 0 & \beta\frac{\Lambda_h}{\mu_h}\\ \alpha_t & c_{55}-\xi & 0\\ p_i & p_c & (r-\mu_b)-\xi \end{pmatrix}=0,$$

$$\det\begin{pmatrix} c_{22}-\xi & \alpha_{mh}b_m\\ h_4 & -\mu_m-\xi \end{pmatrix}=0.$$

It can be shown that all five solutions of these equations have negative real part if $\mathcal{R}_0^T<1$ and $\mathcal{R}_0^M<1$ (see Appendices A and B). This shows that all eigenvalues of $\mathbf{J}$ have negative real part if $\mathcal{R}_0<1$. Hence, the local stability of $\mathcal{E}_0$ can be determined by $\mathcal{R}_0$. □

We also performed thorough analysis of corresponding single disease models (see Appendix A and Appendix B), including our novel typhoid fever model. We found that R_0^T and R_0^M correspond to the typhoid and malaria basic reproduction number, respectively. Our analyses identified distinct characteristics of these two dynamical systems governing malaria infections and typhoid infections. We found that the global dynamics of typhoid infection can be determined by a single threshold $\mathcal{R}_0^T$, i.e. $\mathcal{R}_0^T<1$ ($\mathcal{R}_0^T>1$) provides conditions for the global eradication (uniform persistence) of typhoid infection (Theorem 2, Appendix A). However, we need two thresholds—$\mathcal{R}_0^M$ and $\mathcal{R}_0^{MM}$ (the extinction index)—to determine the global dynamics of malaria infection. In malaria infection dynamics, $\mathcal{R}_0^M<\mathcal{R}_0^{MM}<1$ and $\mathcal{R}_0^{MM}>\mathcal{R}_0^M>1$ give conditions for global eradication and uniform persistence, respectively (Remark 1, Appendix B). In a special case of $\alpha_h=\omega=0$, $\mathcal{R}_0^M=\mathcal{R}_0^{MM}$, which gives a single threshold determining the global dynamics of malaria.

To be consistent with our analysis of single disease models, we presented above only the simplified model. However, we are in fact able to perform the local stability analysis of the disease-free equilibrium for the full system (2.3) (see Appendix C).

4. Malaria–typhoid in Kenya: Illustrative numerical analysis

4.1. Overview

We use our co-infection model (full model) to perform an illustrative numerical analysis of the malaria–typhoid co-infection in the Eastern Province of Kenya. We compute the value of $\mathcal{R}_0$ for Eastern Province of Kenya and study how $\mathcal{R}_0$ can be brought to less than one (i.e. a condition for eradication of both diseases, Theorem 1) by implementing potential prevention programs such as the use of mosquito-nets and the chlorination of water. For our model simulations, we use a period of one epidemic season, i.e. a duration of 100 days. We estimate the disease prevalence, the number of new cases of malaria and typhoid, and the disease-related deaths. For this period we also compute the number of possible false diagnosis as a result of the similar signs and symptoms and as a result of false positive in Widal test.

4.2. Data and assumptions

Kenya is one of the developing countries in the sub-Saharan Africa. It has a population of about 44 million with an estimated growth rate of 2.27% [12]. The country's location and development status put it in the category of regions hardest hit by malaria and typhoid; approximately 74% [25] and 40% [23] of the total population of Kenya are at risk of contracting malaria and typhoid, respectively. In this study, we focus on the Eastern Province, the second largest of the total eight provinces in the country, because of significantly high transmission rate of malaria and typhoid.

We include the entire population in the Eastern Province of Kenya (approximately 5.66 million people) as the initial total population, $N_h(0)$. Parameters are estimated and/or calculated based on literature review (see Table 1). Since some parameters, such as bacteria excretion rates, bacteria death rate, and bacteria growth rate, are not available in the literature, we vary them between some realistic limits. Other parameters are obtained/estimated from the literature and are presented in the time unit of per day. For example, the recovery rate from malaria is found to be 14.12 per year [3], which corresponds to 0.038 per day. All the parameters used for model simulations are given in Table 1.

4.3. The basic reproduction number

Using the mathematical formulas derived above, we now calculate the basic reproduction number, $\mathcal{R}_0$, which represents a threshold condition for the eradication of the diseases. For Eastern Province of Kenya (i.e. using the parameter values in Table 1), we obtain $\mathcal{R}_0^M=2.51$ and $\mathcal{R}_0^T=18.11$, and therefore, $\mathcal{R}_0=\max\{\mathcal{R}_0^T,\mathcal{R}_0^M\}=18.11$. Note that our estimate of the malaria reproduction number, $R_0^M=2.51$, is consistent with the previous estimates [4]. However, we do not have previous knowledge of typhoid reproduction number. In the base case computation, the typhoid reproduction number is higher than the malaria reproduction number in the Eastern Province of Kenya, so the basic reproduction number in the base case is governed by the typhoid disease.

We performed sensitivity analyses of the reproduction number to the parameters used by calculating the sensitivity indices [13]. The sensitivity index of $\mathcal{R}_0^M$ and $\mathcal{R}_0^T$ with respect to a parameter ξ, is given by $\frac{\partial\mathcal{R}_0^M}{\partial\xi}\times\frac{\xi}{\mathcal{R}_0^M}$, $\frac{\partial\mathcal{R}_0^T}{\partial\xi}\times\frac{\xi}{\mathcal{R}_0^T}$. The negative (or positive) sign of the sensitivity index indicates whether the typhoid or malaria reproduction number decreases (or increases) when the corresponding parameter is increased. From the calculated indices (Table 2), we observe that the most sensitive parameters are b_m (for malaria) and μ_b (for typhoid).

Based on our sensitivity analysis, we now consider the parameter, b_m, the average number of mosquito bites, to reflect malaria prevention (for example, mosquito-nets), and the parameter μ_b, the bacteria degradation rate in the environment, to reflect typhoid prevention (for example, chlorination of water), and determine prevention-related conditions under which $\mathcal{R}_0$ is less than one. Using other parameter values fixed as in Table 1, we observe how $\mathcal{R}_0$ changes as a function of b_m and μ_b (Fig. 2a). Moreover, using a contour plot corresponding to $\mathcal{R}_0^T=\mathcal{R}_0^M$, which gives $b_m=f(\mu_b)$, we identify the

Table 1
Malaria–typhoid model parameters and their interpretations.

Description	Parameter	Estimate	Source
Total human population	N_h	5668123	[12]
Total mosquito population	N_m	3400873	Estimate, [4]
Recruitment rate of humans	Λ_h	467 day^{-1}	Calculated, [12]
Recruitment rate of mosquitoes	Λ_m	0.13 $\times$ N_m day^{-1}	Calculated, [4]
Transmission probability for malaria in mosquitoes	α_{hm}	0.000408	Calculated, [4]
Transmission probability for malaria in humans	α_{mh}	0.15096	Calculated, [4]
Maximum number of mosquito bites	b_m	12 day^{-1}	[4]
Natural death rate of humans	μ_h	0.00004 day^{-1}	[12]
Natural death rate of mosquitoes	μ_m	0.033 day^{-1}	[4]
Malaria exposed humans infection rate	δ_h	0.08333 day^{-1}	[27]
Malaria exposed mosquitoes infection rate	γ_m	0.1 day^{-1}	[27]
Recovery rate from malaria	α_h	0.038 day^{-1}	[3,4]
Malaria-induced death rate	ω	0.0019 day^{-1}	Calculated, [4]
Typhoid-induced death rate	λ	0.002 day^{-1}	[30]
Recovery rate from typhoid infection	η	0.0357 day^{-1}	[1]
Rate of progression from infective to carriers	α_t	0.04 day^{-1}	[30]
Recovery rate from carriers	γ	0.000315 day^{-1}	[30]
Infection rate of typhoid	β	1.97 $\times$ 10^{-11} day^{-1}	Calculated, [30]
Bacteria excretion (infected)	p_i	10	Assumed
Bacteria excretion (carriers)	p_c	1	Assumed
Rate at which bacteri become non-infectious	μ_b	0.0345 day^{-1}	Varied
Bacteria reproduction rate in environment	r	0.014 day^{-1}	Assumed
Typhoid increased susceptibility in malaria infections	ψ	1.5 [1-3]	Varied
Slower recovery in malaria	θ	0.5 [0-1]	Varied
Slower recovery in typhoid	σ	0.5 [0-1]	Varied

Table 2
Sensitivity indices.

Description	Parameter	Sensitivity index
Maximum number of mosquito bites	b_m	+1.000
Recovery rate from malaria	α_h	− 0.8088
Natural death rate of mosquitoes	μ_m	− 0.7100
Transmission probability for malaria in mosquitoes	α_{hm}	+0.5000
Transmission probability for malaria in humans	α_{mh}	+0.5000
Malaria-induced death rate	ω	− 0.0404
Natural death rate of humans	μ_h	− 0.0246
Rate at which bacteria in the environment become non-infectious	μ_b	-0.5057
Infection rate of typhoid	β	+0.4943
Recovery rate from typhoid infection	η	− 0.1858
Bacteria reproduction rate in environment	r	+0.0174
Bacteria excretion (carriers)	p_c	+0.0140
Typhoid-induced death rate	λ	− 0.0020
Rate of progression from infective to carriers	α_t	− 0.0020
Bacteria excretion (infected)	p_i	+0.0013

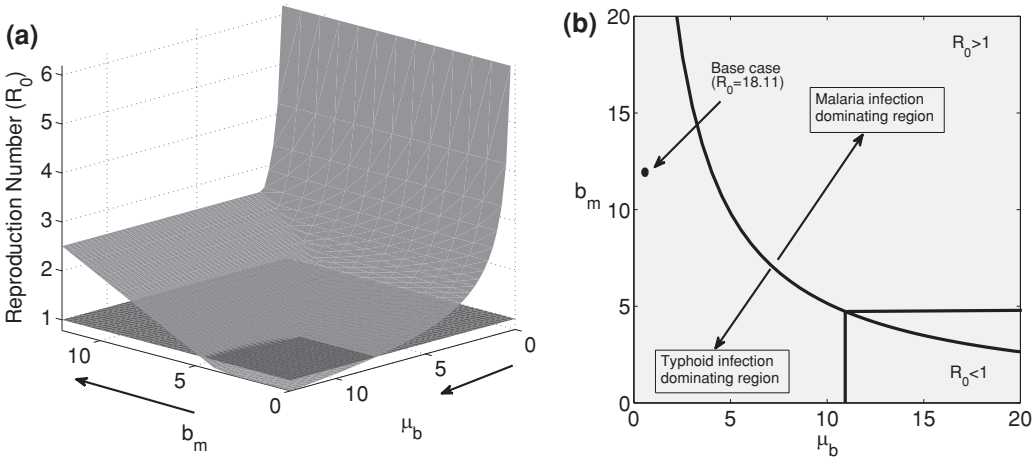

Fig. 2. (a) 3-D plot and (b) contour plot showing how the basic reproduction number depends on b_m, the number of mosquito bites (related to malaria prevention) and μ_b, the rate at which bacteria in the environment become non-infectious (related to typhoid prevention).

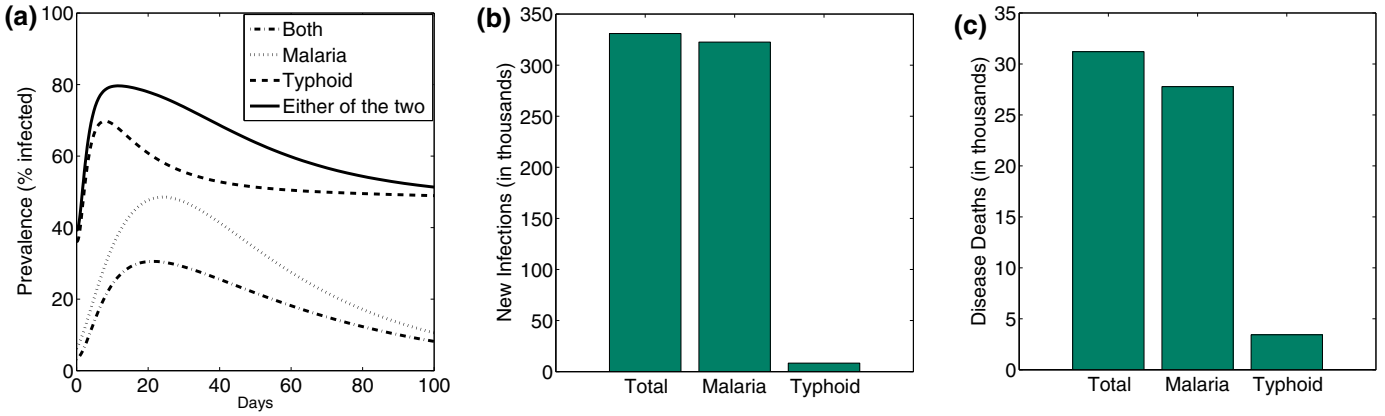

Fig. 3. The prevalence of malaria, typhoid, both, and either of them predicted by the co-infection model and (a) the total number of new infections and (b) the total number of deaths due to malaria and typhoid during one epidemic season (100 days).

regions in $b_m\mu_b$-parameter space, where malaria or typhoid dominates (Fig. 2b). As shown in Fig. 2b, the $b_m\mu_b$-parameter space is divided approximately by the exponentially decaying curve $b_m = f(\mu_b)$, above (below) which the malaria (typhoid) infection dominates. As expected, an increase in μ_b in typhoid dominating region and/or a decrease in b_m in malaria dominating region decrease the value of $\mathcal{R}_0$ eventually reaching the region where $\mathcal{R}_0 < 1$ (Fig. 2). This suggests that the malaria–typhoid co-infection could be controlled theoretically through prevention programs that sufficiently reduce b_m and increase μ_b. For Eastern Province of Kenya, we find that if $b_m < 5$ and $\mu_b > 11$, then $\mathcal{R}_0 < 1$ (Fig. 2).

4.4. Disease outcomes: Prevalence, new infections, and disease deaths

4.4.1. Base case

Fig. 3a shows a time-course of the disease prevalence over a period of 100 days (one epidemic season) predicted by our model. At the end of the epidemic season, the typhoid prevalence reaches 49.2% and the malaria prevalence reaches 10.3% with the total disease prevalence (either malaria or typhoid) of 51.5%. For the entire season, the typhoid remains relatively high prevalent compared to malaria. Importantly, our results show that there is a significantly large portion of individuals co-infected with malaria and typhoid, reaching about 30% within three weeks and approximately 8% at the end of the season. This significant high portion of co-infected populations underscores the need of prevention programs simultaneously focused on both diseases.

4.4.2. Effects of co-infection

Using our model, we calculate the total number of new malaria cases and new typhoid cases as well as the total deaths due to these diseases (Fig. 3b and c). Based on our simulations, we estimate that about 320 thousand new malaria cases and about 10 thousand new typhoid cases occur during one season in the Eastern province of Kenya (Fig. 3b). Similarly, we calculate that the Eastern Province of Kenya suffers from 28 thousand malaria deaths and four thousand typhoid deaths in a single season (Fig. 3c). Our estimates are in agreement with the estimates by Standard Media Kenya [41]. Interestingly, we find that despite the higher prevalence of typhoid, malaria is more problematic in terms of new cases and disease deaths.

In our co-infection dynamics model, effects of one disease on another are represented by the parameters ψ (increased susceptibility of typhoid due to malaria infection), σ (slow recovery from typhoid due to co-infection with malaria), and θ (slow recovery from malaria due to co-infection with typhoid). We now observe how these parameters affect the prevalence, new infections, and disease deaths. We find that the prevalence of malaria, typhoid, and both increases as ψ increases, σ decreases, and/or θ decreases. This is because these conditions lead to more people living with diseases as they provide increased infectivity and decreased recovery and death.

We also find significant effects of ψ on the total typhoid deaths as well as the total typhoid new infections (Fig. 4a and d); an increase in ψ from $\psi = 1$ (no effect) to $\psi = 3$ can increase the typhoid new cases by 70% and the typhoid deaths by 24%. Similarly, a change in σ from 1 (no effect) to 0 (maximum effect) can increase the typhoid death, and the typhoid new infection by 56% and 22%, respectively (Fig. 4b and e). Furthermore, a decrease in θ from 1 (no effect) to 0 (maximum effect) has a significant effect on the total malaria death (from 23 thousand to 40 thousand) (Fig. 4c). However, the malaria new infection is not sensitive to the change in θ (Fig. 4f).

4.5. False diagnosis

4.5.1. Based on signs and symptoms

Diagnosis of diseases based on their signs and symptoms is quite common in resource deprived countries like Kenya. Because of similarity in signs and symptoms between malaria and typhoid, false diagnosis is highly frequent in individuals infected with one of these diseases [36]. To quantify the possible false diagnosis based on signs and symptoms, we introduce a parameter τ, representing the average rate per day at which individuals are diagnosed through the signs and symptoms. Note that individuals in compartment X_{ij}, $i = I$ or $j = I$ are candidates for becoming sick, i.e. showing signs and symptoms. Thus we subtract τX_{ij} from the corresponding equation of the model system (Fig. 1), and then the total number of individuals who are diagnosed based on signs and symptoms is given by $D^{\text{Tot}} = \int_0^{100} \tau (X_{SI} + X_{IS} + X_{IE} + X_{CI} + X_{II} + X_{RI} + X_{IR}) dt$. Among them, the total number of individuals, who may be sick due to malaria is $D^M = \int_0^{100} \tau \left(X_{SI} + X_{CI} + X_{II} + X_{RI}\right) dt$, and who may be sick due to typhoid is $D^T = \int_0^{100} \tau \left(X_{IS} + X_{IE} + X_{II} + X_{IR}\right) dt$. Therefore, possible malaria false diagnosis and typhoid false diagnosis cases based on signs and symptoms are given by $D^{\text{Tot}} - D^M$ and $D^{\text{Tot}} - D^T$, respectively. For $\tau = 1$, we find that about 4.1 million cases can be falsely diagnosed with typhoid while about 1 million cases can be falsely diagnosed with malaria (Fig. 5). These results show that typhoid is likely to have four times higher cases of false diagnosis compared to malaria. As shown in Fig. 5b, a higher value of τ gives a larger number of false diagnosis cases, with the predicted total number of cases being more sensitive to τ when the value of τ is small.

4.5.2. By Widal test

In many parts of the world, including Kenya, Widal test is a commonly used method for typhoid diagnosis. However, this method can give frequent false positive results because of cross-reaction between malaria parasites and typhoid antigens. To calculate the

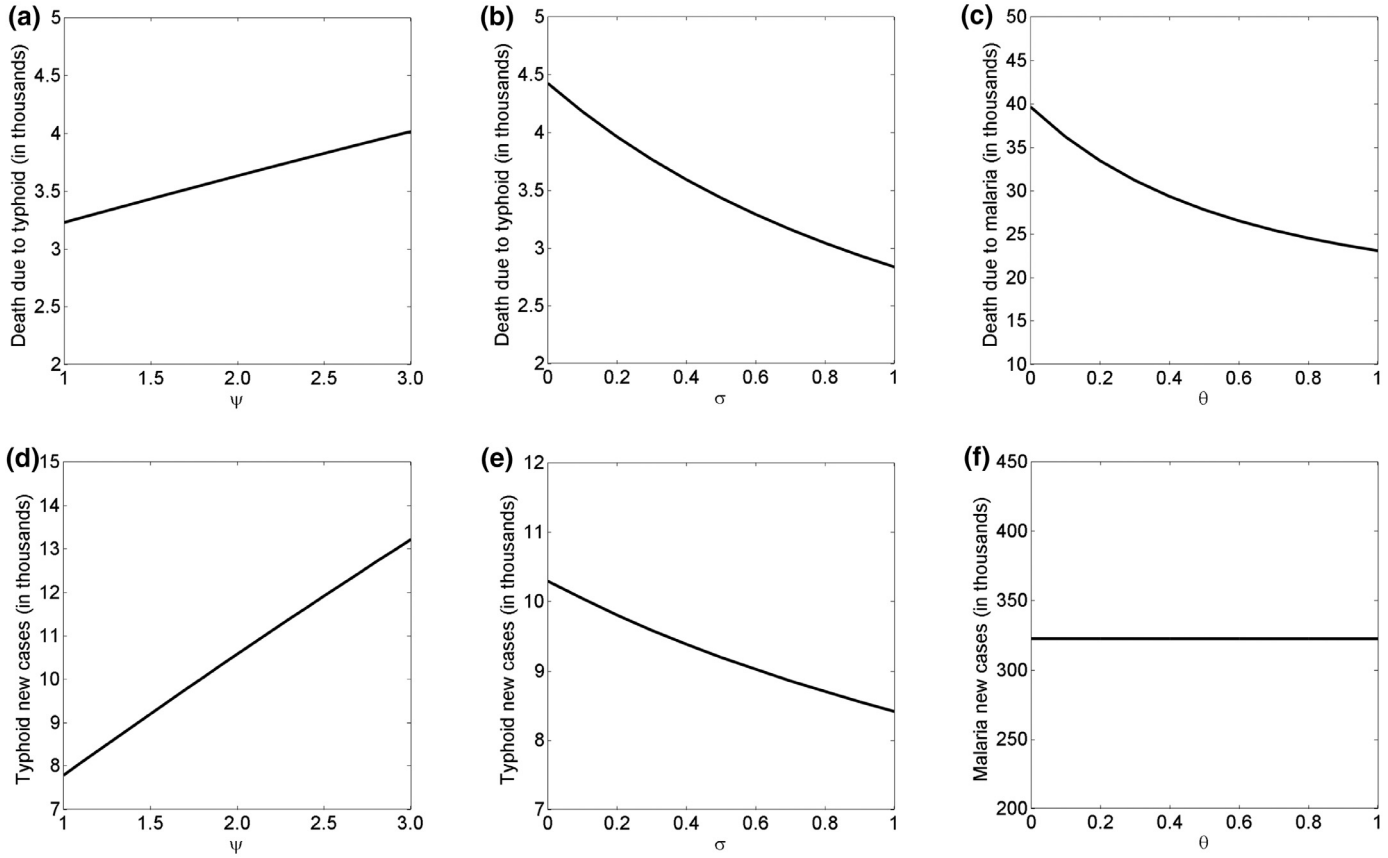

Fig. 4. Effects of co-infection related parameters, namely ψ (increased susceptibility of typhoid due to malaria infection), σ (slow recovery from typhoid due to co-infection with malaria), and θ (slow recovery from malaria due to co-infection with typhoid) on the total new infections and disease deaths during one epidemic season (100 days).

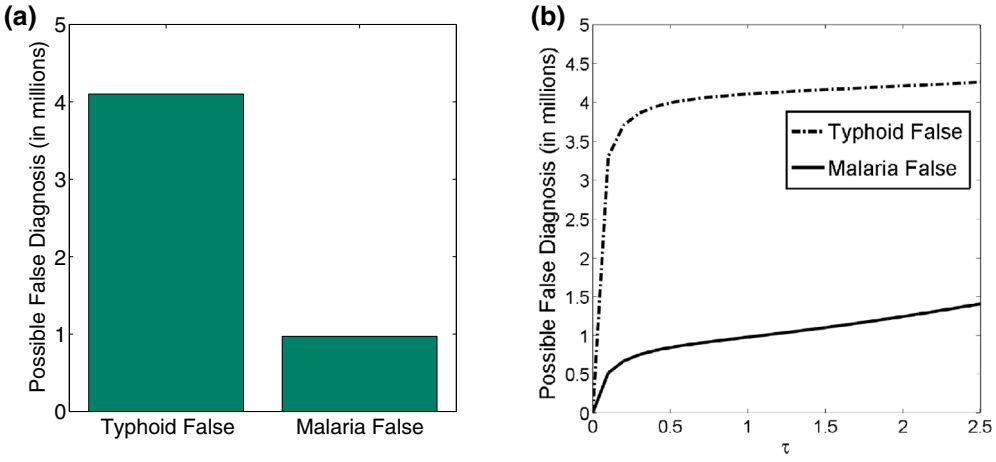

Fig. 5. (a) The number of possible false diagnosis cases based on signs and symptoms during one epidemic season (100 days) and (b) the dependence of the possible false diagnosis cases on the value of τ. τ represents the average rate per day at which individuals are diagnosed through the signs and symptoms. The first figure (base case) corresponds to $\tau = 1$.

possible false positive cases by Widal test, we introduce a parameter ϕ, representing the average rate per day at which individuals are tested for typhoid by Widal test. Following the similar argument as in the calculation of false diagnosis based on signs and symptoms above, the total number of possible false positive cases by Widal test is given by $W^{\text{Tot}} - W^{T}$, where $W^{\text{Tot}} = \int_0^{100} \phi(X_{SI} + X_{IS} + X_{IE} + X_{CI} + X_{II} + X_{RI} + X_{IR})dt$, and $W^{T} = \int_0^{100} \phi\,(X_{IS} + X_{IE} + X_{II} + X_{CI} + X_{IR})\,dt$. Our calculation for $\phi = 1$ shows that among about 5.2 million people having Widal test done, approximately 2 million cases are truly typhoid infected, indicating that there is a possibility of up to 60% typhoid false positive in Widal test (Fig. 6). This result is in agreement with experimental studies in which as high as 57% typhoid positive cases were seen in Widal test results instead of 14% actual positive cases [16]. The total number of possible false positive cases increases as the value of ϕ increases; the increase is particularly pronounced for small values of ϕ (Fig. 6b).

4.6. Sensitivity analysis

Note that we assumed permanent immunity and ignored direct transmission in our model. However, rapid immunity loss from malaria infection and direct (person-to-person) transmission of

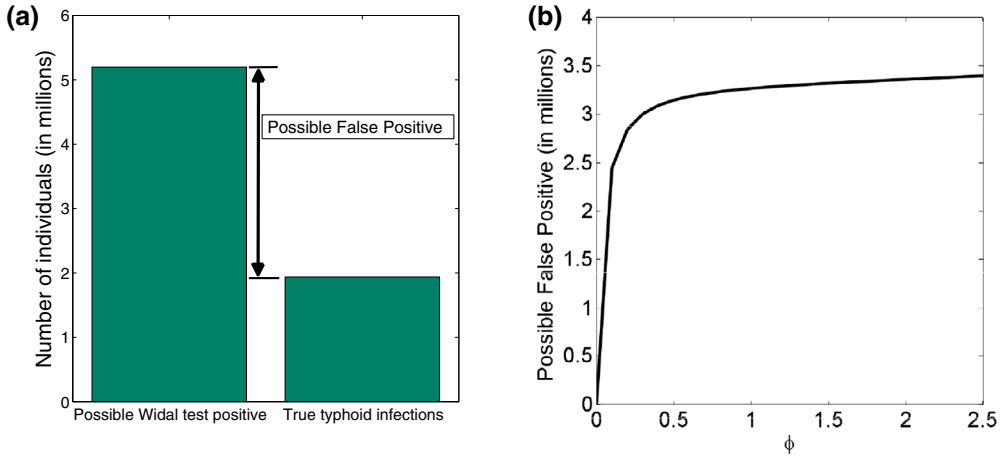

Fig. 6. (a) The total number of possible false positive cases by Widal test during one epidemic season (100 days) and (b) the dependence of the total number of possible Widal test false positive cases on the value of ϕ. ϕ represents the average rate per day at which individuals are tested for typhoid by Widal test. The first figure (base case) corresponds to $\phi = 1$.

typhoid infection have been considered in some studies [3,4,29]. Therefore, in this section we study how our model predictions are affected by introducing these phenomena. First, we introduced the loss of malaria immunity rate into the model, and examined its sensitivity on malaria new infection, death, and the prevalence. If individuals lose immunity in average in 30 days after recovery, the total new infection would rise to more than a double from the base case result and the total disease death increases by 25%. Similarly, the immunity loss rate of 1/60 per day and 1/90 per day would result in 75% and 18% increase in new infections, and 18% and 14% increase in deaths, respectively. The malaria prevalence increases by 29%, 23%, and 18% from the base case for 30, 60, and 90 days of immunity period, respectively, whereas the co-infection prevalence increases by 15%, 11%, and 10%, respectively. We observed that the malaria new infections are more sensitive to the change in immunity loss rate compared to the disease deaths. Importantly, the co-infection prevalence, which is the primary focus of this study, is only slightly affected when the immunity loss is ignored in the model.

We next considered a model that also includes typhoid transmissions by direct person-to-person contacts. Using a previously used value of 0.01 per individual per day [29], we observed that typhoid prevalence would increase from 49.2% (without direct transmission) to 58% and the co-infection prevalence from 8% (without direct transmission) to 10%. This shows that contributions of indirect transmission to this co-infection is significantly higher compared to direct transmission. Thus we expect that our analysis and simulation results are only negligibly affected by ignoring the direct typhoid transmission in the model.

5. Discussion

Malaria and typhoid pose a major public health challenge in the developing countries. The risk of contracting either or both of these diseases is high in the tropics, and so their prevalence has remained high compared to other tropical diseases [44]. Here we develop novel mathematical models to study co-infection dynamics of malaria and typhoid. Our results, based on theoretical model analysis and illustrative numerical analysis in the Eastern Province of Kenya, offer some interesting insights into the underlying association between these two diseases, and may provide helpful information for devising their control strategies.

First, we performed thorough analysis of single disease models, including our novel model for typhoid fever. Our analyses identified distinct characteristics of these two dynamical systems governing malaria infections and typhoid infections. We found that the global dynamics of typhoid infection can be determined by a single threshold $\mathcal{R}_0^T$, the typhoid basic reproduction number, i.e. $\mathcal{R}_0^T < 1$ ($\mathcal{R}_0^T > 1$) provides conditions for the global eradication (uniform persistence) of typhoid infection (Theorem 2). However, we need two thresholds—$\mathcal{R}_0^M$ (the malaria basic reproduction number) and $\mathcal{R}_0^{MM}$ (the extinction index)—to determine the global dynamics of malaria infection. In malaria infection dynamics, $\mathcal{R}_0^M < \mathcal{R}_0^{MM} < 1$ and $\mathcal{R}_0^{MM} > \mathcal{R}_0^M > 1$ give conditions for global eradication and uniform persistence, respectively (Remark 1, Appendix B. We note that in a special case of $\alpha_h = \omega = 0$, $\mathcal{R}_0^M = \mathcal{R}_0^{MM}$, which gives a single threshold determining the global dynamics of malaria.

We derived the basic reproduction number for the co-infection dynamics as $\mathcal{R}_0 = \max\{\mathcal{R}_0^T, \mathcal{R}_0^M\}$ and established the local stability of the disease free equilibrium (Theorem 1). According to our analysis, the disease free equilibrium of the model is locally asymptotically stable if $\mathcal{R}_0 < 1$, and unstable if $\mathcal{R}_0 > 1$. For the Eastern Province of Kenya, we computed $\mathcal{R}_0 = 18.11 > 1$, showing a disease outbreak in the Eastern Province of Kenya. Using the expression for $\mathcal{R}_0$, we evaluated the effects of potential prevention measures for these diseases; particularly, we observed the effects of key parameters b_m (prevention measure for malaria) and μ_b (prevention measure for typhoid) on $\mathcal{R}_0$ (Fig. 2). Our results suggest that with a strong prevention program that sufficiently reduces the number of mosquito bites (for example, $b_m < 5$) and increases the bacteria degradation rate in the environment (for example, $\mu_b > 11$), these diseases may be successfully controlled in the Eastern Province of Kenya. These results also suggest that for a successful control of malaria–typhoid co-infection, prevention programs that focus on both diseases simultaneously are necessary.

Using our models, we predicted the disease prevalence, and calculated the number of new infections and the disease-related deaths during an epidemic season of 100 days. The co-infection prevalence can reach significantly high (up to 30% at some point) during the season. Moreover, our results indicate that the disease prevalence as well as the total new infections and disease deaths are highly affected by co-infection related parameters (Fig. 4), underscoring the importance of studying malaria typhoid co-epidemics. In this co-epidemic dynamics, one of the interesting results of our study is that although typhoid remains significantly high prevalent throughout the entire season, malaria produces a higher number of new infections and deaths during the season. These paradoxical results are due to longer life of, but less infection by, typhoid infected individuals in the carrier group and/or high infectivity and mortality rate of malaria. This explains

why malaria still remains highly problematic in terms of new infections and disease deaths in developing countries, including Kenya. Furthermore, these results highlight that typhoid carriers constitute an important group in the malaria–typhoid co-epidemics; they may excrete bacteria almost throughout their entire life without showing any signs and symptoms, thereby signifying a high prevalence of typhoid and eventually a high prevalence of co-infection. Therefore, the typhoid carrier group needs to be taken into account while devising control strategies.

Our next observation is related to false diagnosis resulting in potential mismanagement of malaria and typhoid. Diagnoses of malaria and typhoid based solely on clinical signs and symptoms are still commonly practiced in many developing countries, including Kenya, and more importantly, false diagnoses because of the similar signs and symptoms are major obstacles for managing these diseases [2]. Consistent with this, our results show significantly high possible false diagnosis (about 5 million in base case) in this co-infection dynamics, where the typhoid can have four times higher possible false diagnosis cases than malaria. The typhoid false diagnosis can also be concluded from frequent false positive results in Widal test [5,36], a typhoid diagnosis method commonly used because of convenience and inexpensiveness. Significant possible false positive cases (up to 60% in base case) as predicted by our model shows that the results from Widal test should be carefully considered to avoid increased burden in false diagnosis. As clarified by our results, these high rates of false diagnosis due to the similar signs and symptoms and false positiveness by Widal test indicate an urgent need of more reliable and effective diagnosis methods for proper controls of these diseases.

Our study has a few limitations. Limited data exist on the co-infection of malaria and typhoid; particularly modeling study on typhoid is extremely scarce. Therefore, some of our numerical estimates remain uncertain, particularly those that are most sensitive to typhoid-related parameters. We assumed uniform infectivity among individuals in the same compartment, and considered certain forms of infection-incidence based on previous similar studies. More data sets and experimental studies are needed to include more realistic biological processes in the models. We were able to perform only limited analysis on the model. Extensive analysis on the full model may be a possible future work in this direction. As mentioned earlier, one of our main goals in this study is to estimate the likelihood of false diagnosis as a result of similar signs and symptoms and the use of Widal test, rather than to evaluate actual treatment programs. However, actual treatment programs need to be evaluated to properly quantify the adverse effects of such false diagnoses. Expansion of our co-infection model to include combined treatment and prevention measures might give better ideas on mitigating the challenges of malaria–typhoid co-infection.

In summary, our mathematical co-infection models may help policy makers devise better strategies for management of these diseases. The models help identify distinct features of malaria and typhoid dynamics, as well as underlying relationships between these diseases in this co-infection. As demonstrated by our models, co-infection of malaria and typhoid, and their false diagnosis can have devastating impacts on tropical developing countries. For a successful control management of malaria and typhoid, more detailed studies of their co-infections are extremely important.

Acknowledgments

This work was funded by the start-up fund from the University of Missouri-Kansas City (NKV, MoCode: KCS28) and the UMRB grant from the University of Missouri Research Board (NKV, Mocode: KDA91). Research of FBW was supported in part by Ministry of Science and Technology, Taiwan (grant number: MOST 103-2115-M-182-001-MY2). The authors would like to thank two anonymous reviewers for their valuable suggestions.

Appendix A. Analysis of typhoid-only model

From Eq. (3.4), we obtain the following typhoid-only model:

$$\begin{aligned}\frac{dX_{SS}}{dt} &= \Lambda_h - \beta B X_{SS} - \mu_h X_{SS},\\ \frac{dX_{IS}}{dt} &= \beta B X_{SS} - (\mu_h + \lambda + \eta + \alpha_t) X_{IS},\\ \frac{dX_{CS}}{dt} &= \alpha_t X_{IS} - (\mu_h + \gamma) X_{CS},\\ \frac{dB}{dt} &= rB\left(1 - \frac{B}{\kappa}\right) + p_i X_{IS} + p_c X_{CS} - \mu_b B.\end{aligned} \tag{A.1}$$

It then follows from [38, Theorem 5.2.1] that for any $(X_{SS}^0, X_{IS}^0, X_{CS}^0, B^0) \in \mathbb{R}^4_+$, system (A.1) has a unique local nonnegative solution $(X_{SS}(t), X_{IS}(t), X_{CS}(t), B(t))$ through the initial value:

$$(X_{SS}(0), X_{IS}(0), X_{CS}(0), B(0)) = (X_{SS}^0, X_{IS}^0, X_{CS}^0, B^0).$$

Let

$$N_1(t) := X_{SS}(t) + X_{IS}(t) + X_{CS}(t). \tag{A.2}$$

Then $N_1(t)$ satisfies

$$\frac{dN_1(t)}{dt} = \Lambda_h - \mu_h X_{SS} - (\mu_h + \lambda + \eta) X_{IS} - (\mu_h + \gamma) X_{CS},$$

which implies that

$$\frac{dN_1(t)}{dt} \le \Lambda_h - \mu_h N_1(t),$$

and hence,

$$\lim_{t\to\infty} N_1(t) \le \frac{\Lambda_h}{\mu_h}. \tag{A.3}$$

This implies that $N_1(t)$ is ultimately bounded. Next, we show that B is ultimately bounded. From (A.2), (A.3) and the last equation of (A.1), it follows that there exists $t_0 > 0$ and $M > 0$ such that

$$\frac{dB}{dt} \le M + rB\left(1 - \frac{B}{\kappa}\right) - \mu_b B, \quad t \ge t_0. \tag{A.4}$$

We consider the following auxiliary equation,

$$\frac{d\bar{B}}{dt} = M + r\bar{B}\left(1 - \frac{\bar{B}}{\kappa}\right) - \mu_b \bar{B}, \quad t \ge 0. \tag{A.5}$$

By [52, Theorem 2.2.1], it is not hard to see that there exists $\bar{B}^* > 0$ such that

$$\lim_{t\to\infty} \bar{B} = \bar{B}^*. \tag{A.6}$$

By (A.4), (A.5), (A.6), and the comparison principle, it follows that B is ultimately bounded. Thus, the solutions of system (A.1) exist globally on the interval $[0, \infty)$.

A1. Global dynamics of system (A.1)

System (A.1) has exactly one typhoid-free equilibrium

$$E_0 = \left(\frac{\Lambda_h}{\mu_h}, 0, 0, 0\right)$$

and the equations for infectious compartments of the linearized system of Eq. (A.1) at E_0 takes the following form:

$$\begin{aligned}\frac{dX_{IS}}{dt} &= -(\mu_h+\lambda+\eta+\alpha_t)X_{IS}+\beta\frac{\Lambda_h}{\mu_h}B,\\ \frac{dX_{CS}}{dt} &= \alpha_t X_{IS}-(\mu_h+\gamma)X_{CS},\\ \frac{dB}{dt} &= p_i X_{IS}+p_c X_{CS}+(r-\mu_b)B.\end{aligned} \tag{A.7}$$

The spectral bound or the stability modulus of an $n\times n$ matrix M, denoted by $s(M)$, is defined by

$$s(M) := \max\{\mathrm{Re}(\lambda) : \lambda \text{ is an eigenvalue of } M\}.$$

Motivated by (A.7), we define the following matrix:

$$J=\begin{pmatrix}-(\mu_h+\lambda+\eta+\alpha_t) & 0 & \beta\frac{\Lambda_h}{\mu_h}\\ \alpha_t & -(\mu_h+\gamma) & 0\\ p_i & p_c & r-\mu_b\end{pmatrix}. \tag{A.8}$$

Clearly, J is irreducible and has non-negative off-diagonal elements. Then $s(J)$ is a simple eigenvalue of J with a positive eigenvector (see, e.g., [39, Theorem A.5]).

We now use the next generation matrix method [46] in order to compute $\mathcal{R}_0^T$, the typhoid basic reproduction number, which is defined as the average number of secondary typhoid infections caused by one typhoid infectious individual during his or her entire infectious period. We introduce the following matrices:

$$F=\begin{pmatrix}0&0&h_1\\0&0&0\\p_i&p_c&r\end{pmatrix},\quad V=\begin{pmatrix}h_2&0&0\\-\alpha_t&\mu_h+\gamma&0\\0&0&\mu_b\end{pmatrix},$$

where $h_1=\beta\frac{\Lambda_h}{\mu_h}$ and $h_2=\mu_h+\lambda+\eta+\alpha_t$. Note that $J=F-V$. The basic reproduction number corresponds to the spectral radius of FV^{-1},

$$\mathcal{R}_0^T=\rho(FV^{-1}).$$

By direct computations, it follows that

$$FV^{-1}=\begin{pmatrix}0&0&a_{13}\\0&0&0\\a_{31}&a_{32}&a_{33}\end{pmatrix},$$

where $a_{31}=\frac{p_i}{h_2}+\frac{p_c\alpha_t}{h_2(\mu_h+\gamma)}$, $a_{32}=\frac{p_c}{\mu_h+\gamma}$, $a_{13}=\frac{h_1}{\mu_b}$, $a_{33}=\frac{r}{\mu_b}$. The characteristic polynomial of FV^{-1} can be determined by

$$\det(FV^{-1}-\xi I)=-\xi(\xi^2-a_{33}\xi-a_{13}a_{31}),$$

and hence,

$$\mathcal{R}_0^T=\frac{a_{33}+\sqrt{a_{33}^2+4a_{13}a_{31}}}{2}.$$

The following is a general result showing that the local stability of the typhoid-free equilibrium, E_0, is determined by $\mathcal{R}_0^T$ (see, e.g. [46, Theorem 2]):

Lemma 1. *The following statements hold.*

(i) $\mathcal{R}_0^T=1$ *if and only if* $s(J)=0$;
(ii) $\mathcal{R}_0^T>1$ *if and only if* $s(J)>0$;
(iii) $\mathcal{R}_0^T<1$ *if and only if* $s(J)<0$.

Thus, the typhoid-free equilibrium E_0 is locally asymptotically stable if $\mathcal{R}_0^T<1$, and unstable if $\mathcal{R}_0^T>1$.

As stated in Theorem 2, we can further prove that $R_0^T=1$ also gives the global threshold criteria for typhoid being eradicated from or persistent in the community. To prove this, we let

$$\Omega_0 := \left\{(X_{SS}^0, X_{IS}^0, X_{CS}^0, B^0)\in\mathbb{R}_+^4 : X_{CS}^0>0\right\},$$

and

$$\partial\Omega_0 := \mathbb{R}_+^4\setminus\Omega_0 := \left\{(X_{SS}^0, X_{IS}^0, X_{CS}^0, B^0)\in\mathbb{R}_+^4 : X_{CS}^0=0\right\}.$$

Theorem 2. *The following statements hold.*

(i) *If $\mathcal{R}_0^T<1$, then the disease-free equilibrium E_0 is globally attractive in $\mathbb{R}_+^4$ for (A.1);*
(ii) *If $\mathcal{R}_0^T>1$, then system (A.1) is uniformly persistent with respect to $(\Omega_0, \partial\Omega_0)$ in the sense that there is a positive constant $\zeta>0$ such that every solution $(X_{SS}(t), X_{IS}(t), X_{CS}(t), B(t))$ of (A.1) with $(X_{SS}(0), X_{IS}(0), X_{CS}(0), B(0))\in\Omega_0$ satisfies*

$$\liminf_{t\to\infty} X_{CS}(t)\geq\zeta. \tag{A.9}$$

Furthermore, system (A.1) admits at least one (componentwise) positive equilibrium.

Proof. Assume that $\mathcal{R}_0^T<1$. It then follows from Lemma 1 (iii) that $s(J)<0$. Thus, there exists a sufficiently small positive number ρ_0 such that $s(J_{\rho_0})<0$ (see, e.g., [24, Section II.5.8]), where

$$J_{\rho_0}=\begin{pmatrix}-(\mu_h+\lambda+\eta+\alpha_t) & 0 & \beta\left(\frac{\Lambda_h}{\mu_h}+\rho_0\right)\\ \alpha_t & -(\mu_h+\gamma) & 0\\ p_i & p_c & r-\mu_b\end{pmatrix} \tag{A.10}$$

is irreducible and has non-negative off-diagonal elements. From (A.2) and (A.3), it follows that there is a $t_1>0$ such that

$$X_{SS}(t)\leq\frac{\Lambda_h}{\mu_h}+\rho_0,\quad\forall\, t\geq t_1.$$

It then follows from the last three equations of (A.1) that

$$\begin{aligned}\frac{dX_{IS}}{dt} &\leq -(\mu_h+\lambda+\eta+\alpha_t)X_{IS}+\beta\left(\frac{\Lambda_h}{\mu_h}+\rho_0\right)B,\quad t\geq t_1,\\ \frac{dX_{CS}}{dt} &= \alpha_t X_{IS}-(\mu_h+\gamma)X_{CS},\quad t\geq t_1,\\ \frac{dB}{dt} &\leq p_i X_{IS}+p_c X_{CS}+(r-\mu_b)B,\quad t\geq t_1.\end{aligned} \tag{A.11}$$

Consider the following auxiliary system

$$\begin{aligned}\frac{dX_{IS}}{dt} &= -(\mu_h+\lambda+\eta+\alpha_t)X_{IS}+\beta\left(\frac{\Lambda_h}{\mu_h}+\rho_0\right)B,\quad t\geq t_1,\\ \frac{dX_{CS}}{dt} &= \alpha_t X_{IS}-(\mu_h+\gamma)X_{CS},\quad t\geq t_1,\\ \frac{dB}{dt} &= p_i X_{IS}+p_c X_{CS}+(r-\mu_b)B,\quad t\geq t_1.\end{aligned} \tag{A.12}$$

Since J_{ρ_0} is irreducible and has non-negative off-diagonal elements, it follows that $s(J_{\rho_0})$ is simple and associates a strongly positive eigenvector $\tilde{v}\in\mathbb{R}^3$ (see, e.g., [39, Theorem A.5]). For any solution $(X_{SS}(t), X_{IS}(t), X_{CS}(t), B(t))$ of (A.1) with nonnegative initial value $(X_{SS}(0), X_{IS}(0), X_{CS}(0), B(0))$, there is a sufficiently large $b>0$ such that $(X_{IS}(t_1), X_{CS}(t_1), B(t_1))\leq b\tilde{v}$ holds. It is easy to see that $V(t) := be^{s(J_{\rho_0})(t-t_1)}\tilde{v}$ is a solution of (A.12) with $V(t_1) := b\tilde{v}$. By the comparison principle [39, Theorem B.1], it follows that

$$(X_{IS}(t), X_{CS}(t), B(t))\leq be^{s(J_{\rho_0})(t-t_1)}\tilde{v},\quad\forall\, t\geq t_1.$$

Since $s(J_{\rho_0})<0$, it follows that

$$\lim_{t\to\infty}(X_{IS}(t), X_{CS}(t), B(t))=(0,0,0).$$

It then follows that the equation for X_{SS} is asymptotic to the following system:

$$\frac{dX_{SS}(t)}{dt}=\Lambda_h-\mu_h X_{SS}(t), \tag{A.13}$$

and hence,

$$\lim_{t\to\infty} X_{SS}(t) = \frac{\Lambda_h}{\mu_h}, \tag{A.14}$$

by the theory for asymptotically autonomous semiflows (see, e.g., [42, Corollary 4.3]). Thus, Part (i) is proved.

Assume that $\mathcal{R}_0^T > 1$. It then follows from Lemma 1 (ii) that $s(J) > 0$. Suppose $\Phi(t)P$ is the solution maps generated by system (A.1) with initial value P. Clearly, the system $\{\Phi(t)\}_{t\geq 0}$ admits a global attractor in $\mathbb{R}^4_+$. Now we prove that $\{\Phi(t)\}_{t\geq 0}$ is uniformly persistent with respect to $(\Omega_0, \partial\Omega_0)$. Given any $(X^0_{SS}, X^0_{IS}, X^0_{CS}, B^0) \in \Omega_0$, it follows from the first equation of system (A.1) that

$$X_{SS}(t) = e^{-\int_0^t A(s_1)ds_1}\left[\Lambda_h \int_0^t e^{\int_0^{s_2} A(s_1)ds_1} ds_2 + X^0_{SS}\right], \tag{A.15}$$

where $A(t) := \beta B(t) + \mu_h \geq \mu_h > 0$. Thus, $X_{SS}(t) > 0, \forall\, t > 0$. By [38, Theorem 4.1.1] as generalized to nonautonomous systems, the irreducibility of the cooperative matrix

$$\begin{pmatrix} -(\mu_h+\lambda+\eta+\alpha_t) & 0 & \beta X_{SS}(t) \\ \alpha_t & -(\mu_h+\gamma) & 0 \\ p_i & p_c & r\left(1-\frac{B(t)}{\kappa}\right)-\mu_b \end{pmatrix}.$$

implies that

$$(X_{IS}(t), X_{CS}(t), B(t)) \gg 0, \quad \forall\, t > 0. \tag{A.16}$$

Thus, both $\mathbb{R}^4_+$ and Ω_0 are positively invariant. Clearly, $\partial\Omega_0$ is relatively closed in $\mathbb{R}^4_+$.

Set $M_\partial := \{P \in \partial\Omega_0 \colon \Phi(t)P \in \partial\Omega_0, \forall\, t \geq 0\}$ and $\omega(P)$ be the omega limit set of the orbit $O^+(P) := \{\Phi(t)P \colon t \geq 0\}$. We can then prove the following claim:

Claim 1: $\omega(P) = \{E_0\}, \forall\, P \in M_\partial$.

Proof of Claim 1: Since $P \in M_\partial$, we have $\Phi(t)P \in M_\partial, \forall\, t \geq 0$, that is, $X_{CS}(t) = 0, \forall\, t \geq 0$. Substituting $X_{CS}(t) = 0, \forall\, t \geq 0$, into the third equation of (A.1), it follows that $X_{IS}(t) = 0, \forall\, t \geq 0$. From the second equation of (A.1), it follows that $\beta B(t) X_{SS}(t) = 0, \forall\, t \geq 0$, and hence, $B(t) = 0, \forall\, t \geq 0$. Then, $X_{SS}(t)$ satisfies the Eq. (A.13), and hence, (A.14) is true. Thus, the claim 1 is valid.

Since $s(J) > 0$, there exists a sufficiently small positive number σ_0 such that $s(J_{\sigma_0}) > 0$ (see, e.g., [24, Section II.5.8]), where

$$J_{\sigma_0} = \begin{pmatrix} -(\mu_h+\lambda+\eta+\alpha_t) & 0 & \beta\left(\frac{\Lambda_h}{\mu_h}-\sigma_0\right) \\ \alpha_t & -(\mu_h+\gamma) & 0 \\ p_i & p_c & r-\mu_b-\frac{r}{\kappa}\sigma_0 \end{pmatrix}$$

is irreducible and has non-negative off-diagonal elements. We now prove the following claim:

Claim 2: E_0 is a uniform weak repeller for $\Phi(t)$ in the sense that

$$\limsup_{t\to\infty} \|\Phi(t)P - E_0\| \geq \sigma_0, \quad \forall\, P \in \Omega_0.$$

Proof of Claim 2: Suppose, by contradiction, there exists $P_0 \in \Omega_0$ such that

$$\limsup_{t\to\infty} \|\Phi(t)P_0 - E_0\| < \sigma_0.$$

Thus, there exists $t_2 > 0$ such that

$$X_{SS}(t) \geq \frac{\Lambda_h}{\mu_h} - \sigma_0 \text{ and } B(t) \leq \sigma_0, \quad \forall\, t \geq t_2.$$

It then follows from the last three equations of (A.1) that

$$\begin{aligned} \frac{dX_{IS}}{dt} &\geq -(\mu_h+\lambda+\eta+\alpha_t)X_{IS} + \beta\left(\frac{\Lambda_h}{\mu_h}-\sigma_0\right)B, \quad t \geq t_2, \\ \frac{dX_{CS}}{dt} &= \alpha_t X_{IS} - (\mu_h+\gamma)X_{CS}, \quad t \geq t_2, \\ \frac{dB}{dt} &\geq p_i X_{IS} + p_c X_{CS} + \left(r-\mu_b-\frac{r}{\kappa}\sigma_0\right)B, \quad t \geq t_2. \end{aligned} \tag{A.17}$$

Consider the following auxiliary system

$$\begin{aligned} \frac{dX_{IS}}{dt} &= -(\mu_h+\lambda+\eta+\alpha_t)X_{IS} + \beta\left(\frac{\Lambda_h}{\mu_h}-\sigma_0\right)B, \quad t \geq t_2, \\ \frac{dX_{CS}}{dt} &= \alpha_t X_{IS} - (\mu_h+\gamma)X_{CS}, \quad t \geq t_2, \\ \frac{dB}{dt} &= p_i X_{IS} + p_c X_{CS} + \left(r-\mu_b-\frac{r}{\kappa}\sigma_0\right)B, \quad t \geq t_2. \end{aligned} \tag{A.18}$$

Since J_{σ_0} is irreducible and has non-negative off-diagonal elements, it follows that $s(J_{\sigma_0})$ is simple and associates a strongly positive eigenvector $\hat{v} \in \mathbb{R}^3$ (see, e.g., [39, Theorem A.5]). By (A.16), it follows that

$$(X_{IS}(t_2), X_{CS}(t_2), B(t_2)) \gg 0.$$

Thus, there is a positive number $\hat{b} > 0$ such that $(X_{IS}(t_2), X_{CS}(t_2), B(t_2)) \geq \hat{b}\hat{v}$ holds. It is easy to see that $\hat{V}(t) := \hat{b}e^{s(J_{\sigma_0})(t-t_2)}\hat{v}$ is a solution of (A.18) with $\hat{V}(t_2) := \hat{b}\hat{v}$. By the comparison principle [39, Theorem B.1], it follows that

$$(X_{IS}(t), X_{CS}(t), B(t)) \geq \hat{b}e^{s(J_{\sigma_0})(t-t_2)}\hat{v}, \quad \forall\, t \geq t_2.$$

Since $s(J_{\sigma_0}) > 0$, it follows that

$$\lim_{t\to\infty} X_{IS}(t) = \lim_{t\to\infty} X_{CS}(t) = \lim_{t\to\infty} B(t) = \infty.$$

This contradiction proves the claim 2.

From the above claims, it follows that any forward orbit of $\Phi(t)$ in M_∂ converges to E_0 which is isolated in $\mathbb{R}^4_+$ and $W^s(E_0)\cap\Omega_0 = \emptyset$, where $W^s(E_0)$ is the stable set of E_0 (see [40]). It is obvious that there is no cycle in M_∂ from E_0 to E_0. By [43, Theorem 4.6] (see also [52, Theorem 1.3.1] and [18, Theorem 4.3 and Remark 4.3]), we conclude that system (A.1) is uniformly persistent with respect to $(\Omega_0, \partial\Omega_0)$ in the sense that there is a positive constant $\zeta > 0$ such that (A.9) holds.

By [51, Theorem 2.4] (see also [52, Theorem 1.3.7]), system (A.1) has at least one equilibrium

$(X^*_{SS}, X^*_{IS}, X^*_{CS}, B^*) \in \Omega_0$, and hence, $X^*_{CS} > 0$. Furthermore, it is easy to see that

$$X^*_{IS} = \frac{\mu_h+\gamma}{\alpha_t}X^*_{CS} > 0 \text{ and } B^*X^*_{SS} = \frac{(\mu_h+\gamma)}{\beta\alpha_t(\mu_h+\lambda+\eta+\alpha_t)}X^*_{CS} > 0.$$

Thus, $(X^*_{SS}, X^*_{IS}, X^*_{CS}, B^*)$ is a (componentwise) positive equilibrium of system (A.1). This completes the proof. □

A2. Uniqueness of endemic equilibrium for typhoid-only model (A.1)

Assume that $\mathcal{R}_0^T > 1$. Then it follows from Theorem 2 (ii) that system (A.1) has a positive equilibrium $(X^*_{SS}, X^*_{IS}, X^*_{CS}, B^*)$, which is obtained by solving

$$\begin{aligned} X^*_{IS} &= Q_1 X^*_{CS}, \\ \beta B^* X^*_{SS} &= Q_2 X^*_{CS}, \\ \Lambda_h - \beta B^* X^*_{SS} - \mu_h X^*_{SS} &= 0, \\ rB^*\left(1-\frac{B^*}{\kappa}\right) + p_i X^*_{IS} + p_c X^*_{CS} - \mu_b B^* &= 0, \end{aligned} \tag{A.19}$$

where

$$Q_1 = \frac{\mu_h+\gamma}{\alpha_t}, \quad Q_2 = \frac{(\mu_h+\gamma)}{\alpha_t(\mu_h+\lambda+\eta+\alpha_t)}. \tag{A.20}$$

From the second and third equations of (A.19), it follows that

$$\Lambda_h - Q_2 X^*_{CS} - \mu_h X^*_{SS} = 0,$$

and hence

$$X^*_{SS} = \frac{1}{\mu_h}[\Lambda_h - Q_2 X^*_{CS}]. \tag{A.21}$$

Then the second equation of (A.19) implies that

$$B^* = \frac{Q_2\mu_h X^*_{CS}}{\beta(\Lambda_h - Q_2 X^*_{CS})}. \tag{A.22}$$

Substituting $X^*_{IS} = Q_1 X^*_{CS}$ and (A.22) into the last equation of (A.19) and simplifying, we obtain

$$G(X^*_{CS}) = 0,$$

where

$$G(X^*_{CS}) = r\mu_h Q_2 \left[\beta(\Lambda_h - Q_2 X^*_{CS}) - \frac{1}{\kappa}\mu_h Q_2 X^*_{CS}\right] - \mu_b \mu_h Q_2 \beta(\Lambda_h - Q_2 X^*_{CS}) + Q_3 \beta^2 (\Lambda_h - Q_2 X^*_{CS})^2,$$
$$Q_3 = p_i Q_1 + p_c.$$

Here, $G(X^*_{CS})$ is a quadratic function and G is concave upward. Note that

$$G(\Lambda_h/Q_2) = -\frac{1}{\kappa} r\mu_h^2 Q_2 \Lambda_h < 0 \tag{A.23}$$

and

$$G(0) = \Lambda_h \beta [Q_3 \Lambda_h \beta + (r - \mu_b)\mu_h Q_2] \tag{A.24}$$

If $G(0) < 0$, then $G(X^*_{CS}) = 0$ has exactly one positive root that is larger than Λ_h/Q_2. This contradicts the positivity of $B*$ in (A.22). If $G(0) > 0$, then $G(X^*_{CS}) = 0$ has exactly two positive roots, one of them is less than Λ_h/Q_2 and the other one is greater than Λ_h/Q_2. Again, the root that is greater than Λ_h/Q_2 contradicts the positivity of $B*$, and $G(X^*_{CS}) = 0$ has at most one positive root that is less than Λ_h/Q_2. Therefore, we conclude that if $\mathcal{R}_0^T > 1$, then system (A.1) has exactly one positive equilibrium.

Appendix B. Analysis of malaria-only model

From Eq. (3.4), we obtain the malaria-only model as

$$\begin{aligned}
\frac{dX_{SS}}{dt} &= \Lambda_h - \frac{\alpha_{mh} b_m X_{SS}}{N_h} I_m - \mu_h X_{SS},\\
\frac{dX_{SI}}{dt} &= \frac{\alpha_{mh} b_m X_{SS}}{N_h} I_m - (\mu_h + \alpha_h + \omega) X_{SI},\\
\frac{dS_m}{dt} &= \Lambda_m - \frac{\alpha_{hm} b_m S_m}{N_h} X_{SI} - \mu_m S_m,\\
\frac{dI_m}{dt} &= \frac{\alpha_{hm} b_m S_m}{N_h} X_{SI} - \mu_m I_m,
\end{aligned} \tag{B.1}$$

where

$$N_h(t) := X_{SS}(t) + X_{SI}(t). \tag{B.2}$$

It then follows from [38, Theorem 5.2.1] that for any $(X^0_{SS}, X^0_{SI}, S^0_m, I^0_m) \in \mathbb{R}^4_+$, system (B.1) has a unique local nonnegative solution $(X_{SS}(t), X_{SI}(t), S_m(t), I_m(t))$ through the initial value:

$$(X_{SS}(0), X_{SI}(0), S_m(0), I_m(0)) = (X^0_{SS}, X^0_{SI}, S^0_m, I^0_m).$$

From (B.2), it follows that $N_h(t)$ satisfies

$$\frac{dN_h(t)}{dt} = \Lambda_h - \mu_h X_{SS} - (\mu_h + \alpha_h + \omega) X_{SI},$$

which implies that

$$\frac{dN_h(t)}{dt} \le \Lambda_h - \mu_h N_h(t),$$

and

$$\frac{dN_h(t)}{dt} \ge \Lambda_h - (\mu_h + \alpha_h + \omega) N_h(t).$$

Thus,

$$\limsup_{t\to\infty} N_h(t) \le \frac{\Lambda_h}{\mu_h}. \tag{B.3}$$

and

$$\liminf_{t\to\infty} N_h(t) \ge \frac{\Lambda_h}{\mu_h + \alpha_h + \omega}. \tag{B.4}$$

Also, $N_m(t) = S_m(t) + I_m(t)$ satisfies

$$\frac{dN_m(t)}{dt} = \Lambda_m - \mu_m N_m \quad \Rightarrow \lim_{t\to\infty} N_m(t) = \frac{\Lambda_m}{\mu_m}.$$

Therefore, N_h and N_m are ultimately bounded, and the solutions of system (B.1) exist globally on the interval $[0, \infty)$.

B1. Persistence of malaria

System (B.1) has exactly one disease-free equilibrium

$$\tilde{E}_0 = \left(\frac{\Lambda_h}{\mu_h}, 0, \frac{\Lambda_m}{\mu_m}, 0\right)$$

and the equations for infectious compartments of the linearized system of model (B.1) at $\tilde{E}_0$ takes the following form:

$$\begin{aligned}
\frac{dX_{SI}}{dt} &= -(\mu_h + \alpha_h + \omega) X_{SI} + \alpha_{mh} b_m I_m,\\
\frac{dI_m}{dt} &= \alpha_{hm} b_m \frac{\Lambda_m}{\mu_m} \frac{\mu_h}{\Lambda_h} X_{SI} - \mu_m I_m.
\end{aligned} \tag{B.5}$$

Motivated by (B.5), we define the following matrix:

$$\tilde{J} = \begin{pmatrix} -(\mu_h + \alpha_h + \omega) & \alpha_{mh} b_m \\ \alpha_{hm} b_m \frac{\Lambda_m}{\mu_m} \frac{\mu_h}{\Lambda_h} & -\mu_m \end{pmatrix}. \tag{B.6}$$

Clearly, $\tilde{J}$ is irreducible and has non-negative off-diagonal elements. Then $s(\tilde{J})$ is a simple eigenvalue of $\tilde{J}$ with a positive eigenvector (see, e.g., [39, Theorem A.5]).

Similar to the typhoid-only case, we compute $\mathcal{R}_0^M$, the malaria basic reproduction number, by using the next generation matrix approach [46]. We introduce the following matrices:

$$\tilde{F} = \begin{pmatrix} 0 & h_3 \\ h_4 & 0 \end{pmatrix}, \quad \tilde{V} = \begin{pmatrix} h_5 & 0 \\ 0 & \mu_m \end{pmatrix},$$

where $h_3 = \alpha_{mh} b_m$ and $h_4 = \alpha_{hm} b_m \frac{\Lambda_m}{\mu_m} \frac{\mu_h}{\Lambda_h}$ and $h_5 = \mu_h + \alpha_h + \omega$. Note that $\tilde{J} = \tilde{F} - \tilde{V}$. The basic reproduction number corresponds to the spectral radius of $\tilde{F}\tilde{V}^{-1}$,

$$\mathcal{R}_0^M = \rho(\tilde{F}\tilde{V}^{-1}).$$

By direct computations, it follows that

$$\tilde{F}\tilde{V}^{-1} = \begin{pmatrix} 0 & \frac{h_3}{\mu_m} \\ \frac{h_4}{h_5} & 0 \end{pmatrix},$$

and hence,

$$\mathcal{R}_0^M = \sqrt{\frac{h_3 h_4}{h_5 \mu_m}}.$$

The following is a general result that the local stability of the disease-free equilibrium $\tilde{E}_0$ is determined by $\mathcal{R}_0^M$ (see, e.g. [46, Theorem 2]):

Lemma 2. *The following statements hold.*

(i) $\mathcal{R}_0^M = 1$ *if and only if* $s(\tilde{J}) = 0$;
(ii) $\mathcal{R}_0^M > 1$ *if and only if* $s(\tilde{J}) > 0$;
(iii) $\mathcal{R}_0^M < 1$ *if and only if* $s(\tilde{J}) < 0$.

Thus, the disease-free equilibrium $\tilde{E}_0$ is locally asymptotically stable if $\mathcal{R}_0^M < 1$, and unstable if $\mathcal{R}_0^M > 1$.

Let

$$\tilde{\Omega}_0 := \left\{(X^0_{SS}, X^0_{SI}, S^0_m, I^0_m) \in \mathbb{R}^4_+ : I^0_m > 0\right\},$$

and

$$\partial\tilde{\Omega}_0 := \mathbb{R}^4_+ \setminus \tilde{\Omega}_0 := \left\{(X^0_{SS}, X^0_{SI}, S^0_m, I^0_m) \in \mathbb{R}^4_+ : I^0_m = 0\right\}.$$

Theorem 3. *Let $\mathcal{R}_0^M > 1$. Then the system (B.1) is uniformly persistent with respect to $(\tilde{\Omega}_0, \partial\tilde{\Omega}_0)$ in the sense that there is a positive constant $\tilde{\zeta} > 0$ such that every solution $(X_{SS}(t), X_{SI}(t), S_m(t), I_m(t))$ of (B.1) with $(X_{SS}(0), X_{SI}(0), S_m(0), I_m(0)) \in \tilde{\Omega}_0$ satisfies*

$$\liminf_{t\to\infty} I_m(t) \geq \tilde{\zeta}. \tag{B.7}$$

Furthermore, system (B.1) admits at least one (componentwise) positive equilibrium.

Proof. Assume that $\mathcal{R}_0^M > 1$. It then follows from Lemma 2 (ii) that $s(\tilde{J}) > 0$. Suppose $\tilde{\Phi}(t)P$ is the solution maps generated by (B.1) with initial value P. Clearly, the system $\{\tilde{\Phi}(t)\}_{t\geq 0}$ admits a global attractor in $\mathbb{R}^4_+$. Now we prove that $\{\tilde{\Phi}(t)\}_{t\geq 0}$ is uniformly persistent with respect to $(\tilde{\Omega}_0, \partial\tilde{\Omega}_0)$. Given any $(X_{SS}^0, X_{SI}^0, S_m^0, I_m^0) \in \tilde{\Omega}_0$, it follows from the first and third equations of system (B.1) that

$$X_{SS}(t) = e^{-\int_0^t \tilde{A}(s_1)ds_1}\left[\Lambda_h \int_0^t e^{\int_0^{s_2}\tilde{A}(s_1)ds_1} ds_2 + X_{SS}^0\right], \tag{B.8}$$

and

$$S_m(t) = e^{-\int_0^t \hat{A}(s_1)ds_1}\left[\Lambda_m \int_0^t e^{\int_0^{s_2}\hat{A}(s_1)ds_1} ds_2 + S_m^0\right], \tag{B.9}$$

where $\tilde{A}(t) := \frac{\alpha_{mh}b_m}{N_h(t)} I_m(t) + \mu_h \geq \mu_h > 0$ and $\hat{A}(t) := \frac{\alpha_{hm}b_m}{N_h(t)} X_{SI}(t) + \mu_m \geq \mu_m > 0$. Thus, $X_{SS}(t) > 0$, and $S_m(t) > 0, \forall\, t > 0$. By [38, Theorem 4.1.1] as generalized to nonautonomous systems, the irreducibility of the cooperative matrix

$$\begin{pmatrix} -(\mu_h+\alpha_h+\omega) & \frac{\alpha_{mh}b_m X_{SS}(t)}{N_h(t)} \\ \frac{\alpha_{hm}b_m S_m(t)}{N_h(t)} & -\mu_m \end{pmatrix}.$$

implies that

$$(X_{SI}(t), I_m(t)) \gg 0, \quad \forall\, t > 0. \tag{B.10}$$

Thus, both $\mathbb{R}^4_+$ and $\tilde{\Omega}_0$ are positively invariant. Clearly, $\partial\tilde{\Omega}_0$ is relatively closed in $\mathbb{R}^4_+$.

Set $M_\partial := \{P \in \partial\tilde{\Omega}_0 : \tilde{\Phi}(t)P \in \partial\tilde{\Omega}_0, \ \forall\ t \geq 0\}$ and $\omega(P)$ be the omega limit set of the orbit $O^+(P) := \{\tilde{\Phi}(t)P : t \geq 0\}$. We then prove the following claim:

Claim 3: $\omega(P) = \{\tilde{E}_0\}, \ \forall\, P \in M_\partial$.

Proof of Claim 3: Since $P \in M_\partial$, we have $\tilde{\Phi}(t)P \in M_\partial, \ \forall\, t \geq 0$, that is, $I_m(t) = 0, \forall\, t \geq 0$. Substituting $I_m(t) = 0, \forall\, t \geq 0$, into the last equation of (B.1), it follows that $X_{SI}(t) = 0, \forall\, t \geq 0$. Then, $X_{SS}(t)$ satisfies the Eq. (A.13), and hence, (A.14) is true. On the other hand, $S_m(t)$ satisfies

$$\frac{dS_m}{dt} = \Lambda_m - \mu_m S_m,$$

and hence, $\lim_{t\to\infty} S_m(t) = \frac{\Lambda_m}{\mu_m}$. Thus, the claim 3 is valid.

Since $s(\tilde{J}) > 0$, there exists a sufficiently small positive number ρ_0 such that $s(\tilde{J}_{\rho_0}) > 0$ (see, e.g., [24, Section II.5.8]), where

$$\tilde{J}_{\rho_0} = \begin{pmatrix} -(\mu_h+\alpha_h+\omega) & \alpha_{mh}b_m\left[1 - \frac{2\rho_0}{\frac{\Lambda_h}{\mu_h}+\rho_0}\right] \\ \alpha_{hm}b_m\left(\frac{\Lambda_m}{\mu_m} - \rho_0\right)\frac{1}{\frac{\Lambda_h}{\mu_h}+\rho_0} & -\mu_m \end{pmatrix}. \tag{B.11}$$

is irreducible and has non-negative off-diagonal elements. We first prove the following claim.

Claim 4: $\tilde{E}_0$ is a uniform weak repeller for $\tilde{\Phi}(t)$ in the sense that

$$\limsup_{t\to\infty} \|\tilde{\Phi}(t)P - \tilde{E}_0\| \geq \sigma_0, \quad \forall\, P \in \tilde{\Omega}_0.$$

Proof of Claim 4: Suppose, by contradiction, there exists $P_0 \in \tilde{\Omega}_0$ such that

$$\limsup_{t\to\infty} \|\tilde{\Phi}(t)P_0 - \tilde{E}_0\| < \rho_0.$$

This and (B.3) imply that there exists $t_3 > 0$ such that

$$N_h(t) \leq \frac{\Lambda_h}{\mu_h} + \rho_0, \quad X_{SS}(t) \geq \frac{\Lambda_h}{\mu_h} - \rho_0 \quad \text{and}$$
$$S_m(t) \geq \frac{\Lambda_m}{\mu_m} - \rho_0, \quad \forall\, t \geq t_3.$$

Thus,

$$\frac{X_{SS}(t)}{N_h(t)} \geq \frac{\frac{\Lambda_h}{\mu_h} - \rho_0}{\frac{\Lambda_h}{\mu_h} + \rho_0} = 1 - \frac{2\rho_0}{\frac{\Lambda_h}{\mu_h} + \rho_0}, \quad \forall\, t \geq t_3.$$

It then follows from the second and fourth equations of (B.1) that

$$\begin{aligned} \frac{dX_{SI}}{dt} &\geq -(\mu_h+\alpha_h+\omega)X_{SI} + \alpha_{mh}b_m\left[1 - \frac{2\rho_0}{\frac{\Lambda_h}{\mu_h}+\rho_0}\right] I_m, \quad t \geq t_3, \\ \frac{dI_m}{dt} &\geq \alpha_{hm}b_m\left(\frac{\Lambda_m}{\mu_m} - \rho_0\right)\left[1\Big/\left(\frac{\Lambda_h}{\mu_h}+\rho_0\right)\right] X_{SI} - \mu_m I_m, \quad t \geq t_3. \end{aligned} \tag{B.12}$$

Consider the following auxiliary system

$$\begin{aligned} \frac{dX_{SI}}{dt} &= -(\mu_h+\alpha_h+\omega)X_{SI} + \alpha_{mh}b_m\left[1 - \frac{2\rho_0}{\frac{\Lambda_h}{\mu_h}+\rho_0}\right] I_m, \quad t \geq t_3, \\ \frac{dI_m}{dt} &= \alpha_{hm}b_m\left(\frac{\Lambda_m}{\mu_m} - \rho_0\right)\left[1\Big/\left(\frac{\Lambda_h}{\mu_h}+\rho_0\right)\right] X_{SI} - \mu_m I_m, \quad t \geq t_3. \end{aligned} \tag{B.13}$$

Since $\tilde{J}_{\rho_0}$ is irreducible and has non-negative off-diagonal elements, it follows that $s(\tilde{J}_{\rho_0})$ is simple and associates a strongly positive eigenvector $\tilde{v} \in \mathbb{R}^2$ (see, e.g., [39, Theorem A.5]).

By (B.10), it follows that

$$(X_{SI}(t_3), I_m(t_3)) \gg 0.$$

Thus, there is a positive number $\tilde{b} > 0$ such that $(X_{SI}(t_3), I_m(t_3)) \geq \tilde{b}\tilde{v}$ holds. It is easy to see that $\tilde{V}(t) := \tilde{b}e^{s(\tilde{J}_{\rho_0})(t-t_3)}\tilde{v}$ is a solution of (B.13) with $\tilde{V}(t_3) := \tilde{b}\tilde{v}$. By the comparison principle [39, Theorem B.1], it follows that

$$(X_{SI}(t), I_m(t)) \geq \tilde{b}e^{s(\tilde{J}_{\rho_0})(t-t_3)}\tilde{v}, \quad \forall\, t \geq t_3.$$

Since $s(\tilde{J}_{\rho_0}) > 0$, it follows that

$$\lim_{t\to\infty} X_{SI}(t) = \lim_{t\to\infty} I_m(t) = \infty.$$

This contradiction proves the claim 4.

From the above claims, it follows that any forward orbit of $\tilde{\Phi}(t)$ in M_∂ converges to $\tilde{E}_0$ which is isolated in $\mathbb{R}^4_+$ and $W^s(\tilde{E}_0) \cap \tilde{\Omega}_0 = \emptyset$, where $W^s(\tilde{E}_0)$ is the stable set of $\tilde{E}_0$ (see [40]). It is obvious that there is no cycle in M_∂ from $\tilde{E}_0$ to $\tilde{E}_0$. By [43, Theorem 4.6] (see also [52, Theorem 1.3.1] and [18, Theorem 4.3 and Remark 4.3]), we conclude that system (B.1) is uniformly persistent with respect to $(\tilde{\Omega}_0, \partial\tilde{\Omega}_0)$ in the sense that there is a positive constant $\tilde{\zeta} > 0$ such that (B.7) holds.

By [51, Theorem 2.4] (see also [52, Theorem 1.3.7]), system (B.1) has at least one equilibrium $(X_{SS}^{**}, X_{SI}^{**}, S_m^{**}, I_m^{**}) \in \tilde{\Omega}_0$, and hence, $I_m^{**} > 0$. Furthermore, from a similar argument as above, we get

$$X_{SS}^{**} > 0, \quad X_{SI}^{**} > 0, \quad S_m^{**} > 0.$$

Thus, $(X_{SS}^{**}, X_{SI}^{**}, S_m^{**}, I_m^{**})$ is a (componentwise) positive equilibrium of system (B.1). This completes the proof. □

B2. Global extinction of malaria

In order to study the extinction of malaria in a dynamics given by system (B.1), we define the following matrix:

$$\tilde{J}' = \begin{pmatrix} -(\mu_h+\alpha_h+\omega) & \alpha_{mh}b_m \\ \alpha_{hm}b_m\frac{\Lambda_m}{\mu_m}\frac{\mu_h+\alpha_h+\omega}{\Lambda_h} & -\mu_m \end{pmatrix}. \tag{B.14}$$

Clearly, $\tilde{J}'$ is irreducible and has non-negative off-diagonal elements. Then $s(\tilde{J}')$ is a simple eigenvalue of $\tilde{J}'$ with a positive eigenvector (see, e.g., [39, Theorem A.5]).

Next we define a new index, $\mathcal{R}_0^{MM}$, the extinction index, that plays an important role in the study of extinction. We introduce the following matrices:

$$\tilde{F}' = \begin{pmatrix} 0 & h_3 \\ h_4' & 0 \end{pmatrix}, \quad \tilde{V} = \begin{pmatrix} h_5 & 0 \\ 0 & \mu_m \end{pmatrix},$$

where $h_4' = \alpha_{hm} b_m \frac{\Lambda_m}{\mu_m} \frac{\mu_h+\alpha_h+\omega}{\Lambda_h}$. Note that $\tilde{J}' = \tilde{F}' - \tilde{V}$. Setting

$$\mathcal{R}_0^{MM} = \rho(\tilde{F}'\tilde{V}^{-1}).$$

By direct computations, it follows that

$$\tilde{F}'\tilde{V}^{-1} = \begin{pmatrix} 0 & \frac{h_3}{\mu_m} \\ \frac{h_4'}{h_5} & 0 \end{pmatrix},$$

and hence,

$$\mathcal{R}_0^{MM} = \sqrt{\frac{h_3 h_4'}{h_5 \mu_m}}.$$

From [48, Theorem 2], we have the following result:

Lemma 3. *$\mathcal{R}_0^{MM} < 1$ if and only if $s(\tilde{J}') < 0$*

The following result is concerned with the extinction of system (B.1):

Theorem 4. *If $\mathcal{R}_0^{MM} < 1$, then the disease-free equilibrium $\tilde{E}_0$ is globally attractive in $\mathbb{R}_+^4$ for (B.1).*

Proof. Assume that $\mathcal{R}_0^{MM} < 1$. It then follows from Lemma 3 that $s(\tilde{J}') < 0$. Thus, there exists a sufficiently small positive number ε_0 such that $s(\tilde{J}'_{\epsilon_0}) < 0$ (see, e.g., [24, Section II.5.8]), where

$$\tilde{J}'_{\epsilon_0} = \begin{pmatrix} -(\mu_h+\alpha_h+\omega) & \alpha_{mh} b_m \\ \alpha_{hm} b_m \left(\frac{\Lambda_m}{\mu_m} + \epsilon_0\right) \frac{1}{\frac{\Lambda_h}{\mu_h+\alpha_h+\omega} - \epsilon_0} & -\mu_m \end{pmatrix}. \tag{B.15}$$

is irreducible and has non-negative off-diagonal elements.

From the third equation of (B.1), it is easy to see that

$$\frac{dS_m}{dt} \le \Lambda_m - \mu_m S_m. \tag{B.16}$$

From (B.4) and (B.16), it follows that there is a $t_4 > 0$ such that

$$N_h(t) \ge \frac{\Lambda_h}{\mu_h+\alpha_h+\omega} - \epsilon_0 \text{ and } S_m(t) \le \frac{\Lambda_m}{\mu_m} + \epsilon_0, \quad \forall\, t \ge t_4.$$

It then follows from the second and fourth equations of (B.1) that

$$\begin{aligned} \frac{dX_{SI}}{dt} &\le -(\mu_h+\alpha_h+\omega)X_{SI} + \alpha_{mh} b_m I_m, \quad t \ge t_4, \\ \frac{dI_m}{dt} &\le \alpha_{hm} b_m \left(\frac{\Lambda_m}{\mu_m} + \epsilon_0\right) \frac{1}{\frac{\Lambda_h}{\mu_h+\alpha_h+\omega} - \epsilon_0} X_{SI} - \mu_m I_m, \quad t \ge t_4, \end{aligned} \tag{B.17}$$

where we have used the fact that $\frac{X_{SS}(t)}{N_h(t)} \le 1$, $t \ge 0$. Consider the following auxiliary system

$$\begin{aligned} \frac{dX_{SI}}{dt} &= -(\mu_h+\alpha_h+\omega)X_{SI} + \alpha_{mh} b_m I_m, \quad t \ge t_4, \\ \frac{dI_m}{dt} &= \alpha_{hm} b_m \left(\frac{\Lambda_m}{\mu_m} + \epsilon_0\right) \frac{1}{\frac{\Lambda_h}{\mu_h+\alpha_h+\omega} - \epsilon_0} X_{SI} - \mu_m I_m, \quad t \ge t_4, \end{aligned} \tag{B.18}$$

Since $\tilde{J}'_{\epsilon_0}$ is irreducible and has non-negative off-diagonal elements, it follows that $s(\tilde{J}'_{\epsilon_0})$ is simple and associates a strongly positive eigenvector $\tilde{v}' \in \mathbb{R}_+^2$ (see, e.g., [39, Theorem A.5]).

For any solution $(X_{SS}(t), X_{SI}(t), S_m(t), I_m(t))$ of (B.1) with nonnegative initial value $(X_{SS}(0), X_{SI}(0), S_m(0), I_m(0)) \in \mathbb{R}_+^4$, there is a sufficiently large $b' > 0$ such that $(X_{SI}(t_4), I_m(t_4)) \le b'\tilde{v}'$ holds. It is easy to see that $\tilde{U}(t) := b' e^{s(\tilde{J}'_{\epsilon_0})(t-t_4)}\tilde{v}'$ is a solution of (B.18) with $\tilde{U}(t_4) := b'\tilde{v}'$. By the comparison principle [39, Theorem B.1], it follows that

$$(X_{SI}(t), I_m(t)) \le b' e^{s(\tilde{J}'_{\epsilon_0})(t-t_4)}\tilde{v}', \quad \forall\, t \ge t_4.$$

Since $s(\tilde{J}'_{\epsilon_0}) < 0$, it follows that

$$\lim_{t\to\infty} (X_{SI}(t), I_m(t)) = (0, 0).$$

It then follows the theory for asymptotically autonomous semiflows (see, e.g., [42, Corollary 4.3]) that the equation for X_{SS} is asymptotic to the system (A.13), and hence, (A.14) holds. Similarly, S_m is asymptotic to the following system :

$$\frac{dS_m}{dt} = \Lambda_m - \mu_m S_m,$$

and hence,

$$\lim_{t\to\infty} S_m(t) = \frac{\Lambda_m}{\mu_m}.$$

This completes the proof. □

Remark 1. In this section, we defined $\mathcal{R}_0^M$ and $\mathcal{R}_0^{MM}$. It is easy to see that $\mathcal{R}_0^{MM} > \mathcal{R}_0^M$. Then we have the following results.

(i) From Theorem 3: If $\mathcal{R}_0^{MM} > \mathcal{R}_0^M > 1$, then the system (B.1) is uniformly persistent and system (B.1) admits at least one (componentwise) positive equilibrium.
(ii) From Theorem 4: If $\mathcal{R}_0^M < \mathcal{R}_0^{MM} < 1$, then the disease-free equilibrium $\tilde{E}_0$ is globally attractive in $\mathbb{R}_+^4$ for (B.1).
(iii) If $\alpha_h = \omega = 0$, then $\mathcal{R}_0^{MM} = \mathcal{R}^M$. In this case, a single threshold $\mathcal{R}_0^{MM} = \mathcal{R}^M$ determines the global stability of the malaria transmission dynamics.

Appendix C. Stability analysis of disease-free equilibrium of the full model system (2.3)

Linearizing the full model system (2.3) at its disease-free equilibrium, we obtain the following linear system

$$\begin{aligned} \frac{dX_{SS}}{dt} &= -\mu_h X_{SS} - \beta \frac{\Lambda_h}{\mu_h} B - \alpha_{mh} b_m I_m, \\ \frac{dX_{SE}}{dt} &= -(\mu_h+\delta_h) X_{SE} + \alpha_{mh} b_m I_m, \\ \frac{dX_{SI}}{dt} &= \delta_h X_{SE} + c_{22} X_{SI}, \\ \frac{dX_{SR}}{dt} &= \alpha_h X_{SI} - \mu_h X_{SR}, \\ \frac{dX_{IS}}{dt} &= c_{33} X_{IS} + \beta \frac{\Lambda_h}{\mu_h} B, \\ \frac{dX_{IE}}{dt} &= -(\mu_h+\lambda+\delta_h+\alpha_t+\sigma\eta) X_{IE}, \\ \frac{dX_{II}}{dt} &= \delta_h X_{IE} - (\mu_h+\lambda+\omega+\alpha_t+\sigma\eta+\theta\alpha_h) X_{II}, \\ \frac{dX_{IR}}{dt} &= \theta\alpha_h X_{II} - (\mu_h+\lambda+\alpha_t+\eta) X_{IR}, \\ \frac{dX_{CS}}{dt} &= \alpha_t X_{IS} - (\mu_h+\gamma) X_{CS}, \\ \frac{dX_{CE}}{dt} &= \alpha_t X_{IE} - (\mu_h+\delta_h+\sigma\gamma) X_{CE}, \\ \frac{dX_{CI}}{dt} &= \delta_h X_{CE} + \alpha_t X_{II} - (\mu_h+\omega+\sigma\gamma+\theta\alpha_h) X_{CI}, \\ \frac{dX_{CR}}{dt} &= \theta\alpha_h X_{CI} + \alpha_t X_{IR} - (\mu_h+\gamma) X_{CR}, \end{aligned} \tag{C.1}$$

$$\begin{aligned}
\frac{dX_{RS}}{dt} &= \gamma X_{CS} + \eta X_{IS} - \mu_h X_{RS},\\
\frac{dX_{RE}}{dt} &= \sigma\eta X_{IE} + \sigma\gamma X_{CE} - (\mu_h + \delta_h) X_{RE},\\
\frac{dX_{RI}}{dt} &= \sigma\eta X_{II} + \sigma\gamma X_{CI} + \delta_h X_{RE} - (\mu_h + \alpha_h + \omega) X_{RI},\\
\frac{dX_{RR}}{dt} &= \eta X_{IR} + \gamma X_{CR} + \alpha_h X_{RI} - \mu_h X_{RR},\\
\frac{dB}{dt} &= p_i (X_{IS} + X_{IE} + X_{II} + X_{IR})\\
&\quad + p_c (X_{CS} + X_{CE} + X_{CI} + X_{CR}) + (r - \mu_b) B,\\
\frac{dS_m}{dt} &= -h_4 (X_{SI} + X_{II} + X_{CI} + X_{RI}) - \mu_m S_m,\\
\frac{dE_m}{dt} &= h_4 (X_{SI} + X_{II} + X_{CI} + X_{RI}) - (\mu_m + \gamma_m) E_m,\\
\frac{dI_m}{dt} &= \gamma_m E_m - \mu_m I_m.
\end{aligned}$$

The 6th equation of (C.1) yields that $X_{IE} \to 0$, as $t \to \infty$. Using this limiting value in the 7th and 10th equations of (C.1), we obtain $X_{II} \to 0$ and $X_{CE} \to 0$, as $t \to \infty$. Then the 8th, 11th, and 14th equations of (C.1) imply $X_{IR} \to 0$, $X_{CI} \to 0$, and $X_{RE} \to 0$, respectively, as $t \to \infty$. Furthermore, the 12th and 15th equations of (C.1) provide $X_{CR} \to 0$ and $X_{RI} \to 0$, respectively, as $t \to \infty$. For these reasons, the 6th, 7th, 8th, 10th, 11th, 12th, 14th, and 15th equations of system (C.1) can be dropped for the stability analysis purposes. Then it suffices to consider the following subsystem, which is decoupled from the 1st, 4th, 13th, 16th, and 18th equations of system (C.1):

$$\begin{aligned}
\frac{dX_{IS}}{dt} &= c_{33} X_{IS} + h_1 B,\\
\frac{dX_{CS}}{dt} &= \alpha_t X_{IS} - (\mu_h + \gamma) X_{CS},\\
\frac{dB}{dt} &= p_i X_{IS} + p_c X_{CS} + (r - \mu_b) B,\\
\frac{dX_{SE}}{dt} &= -(\mu_h + \delta_h) X_{SE} + h_3 I_m,\\
\frac{dX_{SI}}{dt} &= \delta_h X_{SE} + c_{22} X_{SI},\\
\frac{dE_m}{dt} &= h_4 X_{SI} - (\mu_m + \gamma_m) E_m,\\
\frac{dI_m}{dt} &= \gamma_m E_m - \mu_m I_m,
\end{aligned} \tag{C.2}$$

where we also changed the order of the equations.

Therefore, the 7-dimensional subsystem with equations corresponding to the variables X_{IS}, X_{CS}, B, X_{SE}, X_{SI}, E_m, and I_m can provide the local stability criteria for the disease-free equilibrium, i.e., the local stability of disease-free equilibrium of the full system (2.3) can be determined by

$$\mathbb{J} = \begin{pmatrix} \mathbb{J}^T & 0_{3\times 4} \\ 0_{4\times 3} & \mathbb{J}^M \end{pmatrix},$$

where

$$\mathbb{J}^T = \begin{pmatrix} c_{33} & 0 & h_1 \\ \alpha_t & -(\mu_h + \gamma) & 0 \\ p_i & p_c & r - \mu_b \end{pmatrix} \quad \text{and}$$

$$\mathbb{J}^M = \begin{pmatrix} -(\mu_h + \delta_h) & 0 & 0 & h_3 \\ \delta_h & c_{22} & 0 & 0 \\ 0 & h_4 & -(\mu_m + \gamma_m) & 0 \\ 0 & 0 & \gamma_m & -\mu_m \end{pmatrix}.$$

Since $\mathbb{J}$ is a diagonal block matrix with diagonal blocks $\mathbb{J}^T$ and $\mathbb{J}^M$, the eigenvalues of $\mathbb{J}$ are given by the eigenvalues of $\mathbb{J}^T$ and $\mathbb{J}^M$. In Appendix A, we showed that all eigenvalues of $\mathbb{J}^T$ have negative real part if $\mathcal{R}_0^T < 1$. Using a similar technique as in Appendix B, we can also show that all eigenvalues of $\mathbb{J}^M$ have negative real part if $\mathcal{R}_0^{\text{Full},M} < 1$, where

$$\mathcal{R}_0^{\text{Full},M} = \sqrt{\frac{h_4 \delta_h}{h_5(\mu_h + \delta_h)} \cdot \frac{h_3 \gamma_m}{\mu_m(\mu_m + \gamma_m)}}.$$

Therefore, all eigenvalues of $\mathbb{J}$ have negative real part if

$$\mathcal{R}_0^{\text{Full}} = \max\{\mathcal{R}_0^T, \mathcal{R}_0^{\text{Full},M}\} < 1.$$

Hence, the disease-free equilibrium is locally asymptotically stable (unstable) if $\mathcal{R}_0^{\text{Full}} < 1$ ($\mathcal{R}_0^{\text{Full}} > 1$). Note that we obtained the simplified model (3.4) assuming a relatively short duration of malaria exposed classes (i.e., $1/\delta_h \ll 1$ and $1/\gamma_m \ll 1$). Implementing the same limiting condition (i.e., $\delta_h \to \infty$ and $\gamma_m \to \infty$) to $\mathcal{R}_0^{\text{Full}}$, we recover $\mathcal{R}_0$ as expected.

References

[1] L.A. Adetunde, Mathematical methods for the dynamics of typhoid fever in kassena-nankana district of upper east region of ghana, J. Mod. Math. Stat. 2 (2) (2008) 45–49.
[2] R. Afoakwah, D.O. Acheampong, J.N. Boampong, M. Sarpong-Baidoo, E.K. Nwaefuna, P.S. Tefe, Typhoid-malaria co-infection in ghana, Eur. J. Exper. Biol. 1 (3) (2011) 1–6.
[3] R. Aguas, L.J. White, R.W. Snow, M.G.M. Gomes, Prospects for malaria eradication in sub-saharan Africa, PLoS ONE 3 (2008) 1–6.
[4] S. Akbari, N.K. Vaidya, L.I. Wahl, The time distribution of sulfadoxine-pyrimethamine protection from malaria, Bull. Math. Biol. 74 (2012) 2733–2751.
[5] H.M. Alhassan, N.N. Shedali, S.B. Manga, K. Abdullahi, K.M. Hamid, Co-infection profile of salmonella typhi and malaria parasite in sokoto-nigeria, Glob.J. Sci. Eng. Technol. 2 (201) (2012) 13–20.
[6] R.M. Anderson, R.M. May, 1991, Infectious Diseases of Humans: Dynamics and Control, Oxford University Press, Oxford.
[7] S. Baker, K.E. Holt, A.C.A. Clements, A. Karkey, A. Arjyal, M.F. Boni, S. Dongol, N. Hammond, S. Koirala, P.T. Duy, T.V. Nga, J.I. Campbell, C. Dolecek, B. Basnyat, G. Dougan, J.J. Farrar, Combined high-resolution genotyping and geospatial analysis reveals modes of endemic urban typhoid fever transmission, Open Biol. 1 (2011) 110008.
[8] H. Bashyam, Surviving malaria, dying of typhoid, J. Exper. Med. 204 (12) (2007) 2774.
[9] N.A. Bishof, T.R. Welch, L.S. Beischel, C4b deficiency: a risk factor for bacteremia with encapsulated organisms, J. Infect. Dis. 162 (1990) 248–250.
[10] C.K. Brian, S. Wahinuddin, Typhoid and malaria co-infection: An interesting finding in the investigation of tropical fever, Malay. J. Med. Sci. 13 (2006) 74–75.
[11] Centers for Disease Control and prevention (CDC), National Center for Emerging and Zoonotic Infectious Diseases, 2013, Atlanta, USA. http://www.cdc.gov/nczved/divisions/dfbmd/diseases/typhoid-fever/technical.html, accessed 31.01.14.
[12] Central Intelligence Agency (CIA), The World Factbook, 2014, USA. https://www.cia.gov/library/publications/the-world-factbook/geos/ke.html, accessed 15.03.14.
[13] N. Chitnis, T. Smith, R. Steketee, A mathematical model for the dynamics of malaria in mosquitoes feeding on a heterogeneous host population, J. Bio. Dyn. 2 (2008) 259–285.
[14] N. Chitnis, D. Hardy, T. Smith, A periodically-forced mathematical model for the seasonal dynamics of malaria in mosquitoes, Bull. Math. Biol. 74 (2012) 1098–1124.
[15] N. Chitnis, J.M. Cushing, J.M. Hyman, Bifurcation analysis of a mathematical model for malaria transmission, SIAM J. Appl. Math. 67 (2006) 24–45.
[16] A.O. Ekesiobi, M. Igbodika, O. Njoku, Co-infection of malaria and typhoid fever in a tropical community, Anim. Res. Int. 5 (3) (2008) 888–891.
[17] H. Fujikawa, A. Kai, S. Morozumi, A new logistic model for escherichia coli growth at constant and dynamic temparatures, Food Microbiol. 21 (2004) 501–509.
[18] W.M. Hirsch, H.L. Smith, X.Q. Zhao, Chain transitivity, attractivity, and strong repellers for semidynamical systems, J. Dynam. Differ. Equat. 13 (2001) 107–131.
[19] I. Iheukwumere, Nwachukwu, N. Chuks, Kanu, A. Mercy, Manifestations, mismanagement and diagnostic challenges of malaria and typhoid fever, Malaria Chem. Contr. Elim. 2 (109) (2013) 38–41, doi:10.4172/2090-2778.1000109.
[20] Iowa department of public health, guide to surveillance, investigation, and reporting - typhoid fever, 2014. USA, http://www.idph.state.ia.us/idph_universalhelp/MainContent.aspx?glossaryInd=0&TOCId=83930F22-5479-45C4-935B-FDBFBB01BF83, accessed 03.12.14.
[21] E.A. Isibor, Co-infection with malaria parasites and salmonella typhi in patients in Benin city, Nigeria, Ann. Biol. Res. 2 (2) (2011) 361–365.
[22] V.K. Juneja, M.V. Melendres, L. Huang, J. Subbiah, H. Thippareddi, Mathematical modelling of growth of salmonella in raw ground beef under isothermal conditions from 10 to 45 °C, Int. J. Food Microbiol. 131 (2009) 106–111.
[23] S. Kariuki, J. Mwituria, A. Munyao, G. Revathi, J. Onsongo, Typhoid is over-reported in Embu and Nairobi, Kenya, Afr. J. Health Sci. 11 (3-4) (2004) 103–110.

[24] T. Kato, 1976, Perturbation Theory for Linear Operators, Springer-Verlag, Berlin Heidelberg.
[25] Kenya medical research institute (kemri), Kenya malaria fact sheet, Kenya, 2014. http://www.kemri.org/index.php/help-desk/search/diseases-a-conditions/29-malaria/113-kenya-malaria-fact-sheet, accessed 15.03.14.
[26] J.C. Koella, R. Antia, Epidemiological models for the spread of anti-malarial resistance, Malaria J. 2 (1) (2003) 1–11.
[27] G.O. Lawi, J.Y.T. Mugisha, N. Omolo-Ongati, Mathematical model for malaria and meningitis co-infection among children, Appl. Math. Sci. 5 (47) (2011) 2337–2359.
[28] G. Macdonald, 1957, The Epidemiology and Control of Malaria, Oxford University Press, London.
[29] S. Mushayabasa, C.P. Bhunu, N.A. Mhlanga, Modeling the transmission dynamics of typhoid in malaria endemic settings, Applicat. Appl. Math.: Int. J. 9 (1) (2014) 121–140.
[30] S. Mushayabasa, Impact of vaccines on controlling typhoid fever in kassena-nankana district of upper east region of ghana: Insights from a mathematical model, J. Mod. Math. Stat. 5 (2) (2011) 54–59.
[31] E. Mweu, M. English, Typhoid fever in children in africa, Trop. Med. Int. Health 13 (4) (2008) 532–540.
[32] R. Naresh, S. Pandey, Modeling the effect of environmental factors on the spread of bacterial disease in an economically structured population, Applicat. Appl. Math.: Int. J. 7 (1) (2012) 426–454.
[33] E. Nsutebu, P. Ndumbe, The widal test for typhoid fever: Is it useful? Afr. Health 23 (2001) 5–9.
[34] N.K. Nyakoe, R.P. Taylor, J.N. Makumi, J.N. Waitumbi, Complement consumption in children with plasmodium falciparum malaria, Malaria J. 8 (7) (2009) 1–8, doi:10.1186/1475-2875-8-7.
[35] R. Pearl, The growth of populations, Q. Rev. Biol. 2 (1927) 532–548.
[36] P. Pradhan, Co-infection of typhoid and malaria, J. Med. Lab. Diag. 2 (3) (2011) 22–26.
[37] C. Ratledge, L.G. Dover, Iron metabolism in pathogenic bacteria, Ann. Rev. Microbiol. 54 (1) (2000) 881.
[38] H.L. Smith, Monotone Dynamical Systems: An Introduction to the Theory of Competitive and Cooperative Systems, vol. 41, American Mathematical Society Providence, RI, 1995.
[39] H.L. Smith, P.E. Waltman, 1995, The Theory of the Chemostat, Cambridge University Press.
[40] H.L. Smith, X.Q. Zhao, Robust persistence for semidynamical systems, Nonlinear Anal. 47 (2001) 6169–6179.
[41] Standard media kenya., malaria cited as top killer disease in kenya, 2014, http://www.standardmedia.co.ke/health/article/2000110569/malaria-cited-as-top-killer-disease-in-kenya, accessed 30.04.14.
[42] H.R. Thieme, Convergence results and a poincare-bendixson trichotomy for asymptotically autonomous differential equations, J. Math. Biol. (1992) 755–763.
[43] H.R. Thieme, Persistence under relaxed point-dissipativity with application to an endemic model, SIAM J. Math. Anal. 24 (1993) 407–435.
[44] C.J. Uneke, Concurrent malaria and typhoid fever in the tropics: the diagnostic challenge and public health implications, J. Vect. Borne Dis. 45 (2008) 133–142.
[45] A.S. Vadasz, P. Vadasz, M.E. Abashar, A.S. Gupthar, Recovery of an oscillatory mode of batch yeast growth in water for a pure culture, Int. J. Food Microbiol. 71 (2001) 219–234.
[46] P.V.d. Driessche, J. Watmough, Reproduction numbers and sub-threshold endemic equilibria for compartmental models of disease transmission, Math. Biosci. 180 (2002) 29–48.
[47] Virginia department of health, Typhoid Fever, USA, 2013. http://www.vdh.Virginia.gov/epidemiology/factsheets/Typhoid_Fever.htm
[48] J. Warren, P. Mastroeni, G. Dougan, M. Noursadeghi, J. Cohen, M.J. Walport, M. Botto, Increased susceptibility of C1q-deficient mice to *salmonella enterica* serover typhimurium infection, Infect. immun. 70 (2) (2002) 551–557.
[49] World health organization (WHO), guidelines for the treatment of malaria, 2nd ed. Geneva, Switzerland, 2010, accessed 01.12.13.
[50] World health organization (WHO), guidelines for the treatment of malaria, Geneva, Switzerland, 2013. http://who.int/topics/typhoid-fever/en/, accessed 01.12.13.
[51] X. Zhao, Uniform persistence and periodic coexistence states in infinite-dimensional periodic semiflows with applications, Can. Appl. Math. Quart. 3 (1995) 473–495.
[52] X.Q. Zhao, 2003, Dynamical Systems in Population Biology, Springer, New York.